

A STUDY OF THE FAST SOLUTION OF THE OCCLUDED RADIOSITY EQUATION*

KENDALL ATKINSON[†] AND DAVID CHIEN[‡]

Abstract. Consider the numerical solution of the radiosity equation over an occluded surface S using a collocation method based on piecewise polynomial interpolation. Hackbusch and Nowak [Numer. Math., 54 (1989) pp. 463–491] proposed a fast method of solution for boundary integral equations, and we consider the application of their method to the collocation solution of the radiosity equation. We give a combined analytical and experimental study of the ‘clustering method’ of Hackbusch and Nowak, yielding further insight into the method.

Key words. Radiosity equation, clustering method, collocation, fast solution method

AMS subject classifications. 65R20, 65F99

1. Introduction. The *radiosity equation* is a mathematical model for the brightness of a collection of one or more surfaces when their reflectivity and emissivity are given. The equation is

$$(1.1) \quad u(P) - \frac{\rho(P)}{\pi} \int_S u(Q)G(P, Q)V(P, Q) dS_Q = E(P), \quad P \in S,$$

with $u(P)$ the “brightness” or *radiosity* at P and $E(P)$ the *emissivity* at $P \in S$. The function $\rho(P)$ gives the *reflectivity* at $P \in S$, with $0 \leq \rho(P) < 1$. In deriving this equation, the reflectivity at any point of $P \in S$ is assumed to be uniform in all directions from P ; and in addition, the diffusion of light from all points $P \in S$ is assumed to be uniform in all directions from P . Such a surface is called a *Lambertian diffuse reflector*. The radiosity equation is used in the approximate solution of the ‘global illumination problem’ of computer graphics; see Cohen and Wallace [9] and Sillion and Puech [21].

The function G is given by

$$(1.2) \quad \begin{aligned} G(P, Q) &= \frac{\cos \theta_P \cos \theta_Q}{|P - Q|^2} \\ &= \frac{[(Q - P) \cdot \mathbf{n}_P][(P - Q) \cdot \mathbf{n}_Q]}{|P - Q|^4}. \end{aligned}$$

In this \mathbf{n}_P is the inner unit normal to S at P , θ_P is the angle between \mathbf{n}_P and $Q - P$, and \mathbf{n}_Q and θ_Q are defined analogously; cf. Figure 1.1. The function $V(P, Q)$ is a “line of sight” function. More precisely, if the points P and Q can “see each other” along a straight line segment which does not intersect S at any other point, then $V(P, Q) = 1$; and otherwise, $V(P, Q) = 0$. An *unoccluded* surface is one for which $V \equiv 1$ on S ; otherwise the surface is called *occluded*.

The numerical solution of the unoccluded case by collocation methods has been studied previously. For example, see [4] for piecewise constant and piecewise linear approximations over unoccluded piecewise smooth surfaces. For an analysis of the effects of edges and corners on the solvability of the radiosity equation and its numerical solution, see [14], [15], and [18]. For a discussion of the numerical integration needed in implementing collocation methods, see [6] and [19]. Note that S need not be connected; and S is usually only piecewise

*Received September 2, 2005. Accepted for publication May 2, 2006. Recommended by F. Stenger.

[†]Dept of Mathematics, University of Iowa, Iowa City, Iowa 52242 (atkinson@math.uiowa.edu).

[‡]Dept of Mathematics, California State University San Marcos, San Marcos, CA 92096 (chien@csusm.edu).

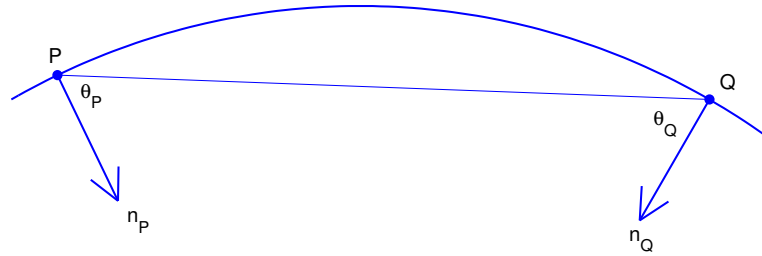


FIG. 1.1. Illustrative graph for defining radiosity kernel (1.2)

smooth. General introductions to the derivation, numerical solution, and application of the radiosity equation (1.1) from a computer graphics perspective can be found in the books [9] and [21].

One of the principal problems in solving (1.2) is the very large operations cost in setting up and solving the large linear systems that arise when discretizing the integral equation. This is true with both Galerkin methods and collocation methods. The matrix coefficients with Galerkin methods are four-fold integrals, and those with collocation methods are two-fold integrals; and near to edges and corners of S , the integrands can be nearly singular. In [5] we proposed and illustrated the use of Hackbusch's clustering method [12] for the solution of the linear system arising with the collocation method in the case that the surface S is unoccluded. In that case, the operations cost is $O(n \log^5 n)$, where n denotes the number of elements into which S is sub-divided in the discretization of the integral equation. The present paper is an analytical and experimental study of the clustering method in the case the surface is occluded. In particular, it is shown that it is not possible to have as good an operations cost as is possible with unoccluded surfaces.

There has been a great deal of work done by researchers from the computer graphics community on rapid methods of solution of discretizations of the radiosity equation. For examples of this, see [10] and [13]. Their perspective is different than that of numerical analysts, who are usually interested in asymptotic rates of convergence regarded as a function of the discretization parameter, and this results in a different way of analyzing operation counts. We comment on this later when our methods are illustrated numerically.

We often write (1.1) in the simpler form

$$(1.3) \quad u(P) - \int_S K(P, Q)u(Q) dS_Q = E(P), \quad P \in S,$$

$$K(P, Q) = \frac{\rho(P)}{\pi} G(P, Q) V(P, Q),$$

or in operator form as

$$(1.4) \quad (I - \mathcal{K})u = E.$$

For a discussion of general stability and convergence results for the collocation solution of this equation, refer to the papers cited above. We note that in general the integral operator \mathcal{K} is not compact for most surfaces S of practical interest, and this has made more difficult the mathematical analysis of collocation methods.

We discuss the triangulation of S and the definition of the collocation method in §2. The clustering method is introduced in §3, and in §4 the error analysis from Hackbusch and Nowak [12] is specialized to the radiosity equation over polyhedral surfaces. In §5 the surface S and true solutions u used in our experiments are introduced, and a very brief description is given of the programs and computing equipment used in the experimental study. In §6 we give our experimental results, discussing the cost as a function of the parameters of the numerical scheme.

2. Triangulation and collocation. We limit our presentation to polyhedral surfaces. The treatment of more general surfaces requires certain nuances which we do not want to consider here; and the problems and methods in which we are interested are illustrated well with polyhedral surfaces. Moreover, many of the surfaces of practical interest are polyhedral.

Our scheme for the triangulation of S is essentially that described in [1, Chap. 5] and implemented in the boundary element package *BIEPACK*, described in [2]. We subdivide the surface S into closed triangular elements $\{\Delta_j\}$ and we approximate u by a low-degree polynomial over each element. We assume there is a sequence of triangulations of S , $\mathcal{T}_n = \{\Delta_{n,k} \mid 1 \leq k \leq n\}$, with some increasing sequence of integer values n , with $n \rightarrow \infty$. In our codes the values of n increase by a factor of 4, due to our method for refining a triangulation. To refine a triangle $\Delta_{n,k}$, we connect the midpoints of its sides, creating four new smaller and congruent triangular elements. There are standard assumptions made on the triangulations. We describe the triangulation process briefly, and the details are left to [1, Chap. 5], [2].

Associated with most surfaces are parameterizations of the surface. We assume the surface S can be written as

$$S = S_1 \cup S_2 \cup \cdots \cup S_J$$

with each S_j a closed polygonal region. Triangulate S_j , say as

$$\{\Delta_{n,k}^j \mid k = 1, \dots, n_j\}.$$

This need not be a ‘conforming triangulation’, in contrast to the situation with finite element methods for solving partial differential equations. For S as a whole, define

$$\mathcal{T}_n = \bigcup_{j=1}^J \{\Delta_{n,k}^j \mid k = 1, \dots, n_j\}.$$

Sometimes we dispense with the subscript n in $\Delta_{n,k}^j$, although it is to be understood implicitly.

We introduce notation and assumptions regarding the mesh size of the triangulations $\{\mathcal{T}_n\}$. The *mesh size* of this triangulation is defined by

$$(2.1) \quad h \equiv h_n = \max_{1 \leq j \leq J} \max_{1 \leq k \leq n_j} \text{diameter}(\Delta_{n,k}^j).$$

As noted earlier, the elements of \mathcal{T}_n are denoted collectively by $\mathcal{T}_n = \{\Delta_{n,k} \mid 1 \leq k \leq n\}$. With each increase of n to $4n$ in our programs, the mesh size h decreases to $\frac{1}{2}h$.

Let $A(\Delta)$ denote the center of the smallest circle (or smallest ball if it is in 3D) containing Δ , $R(\Delta)$ its radius, and $\mu(\Delta)$ its area. Introduce

$$(2.2) \quad \delta_n = \max \{R(\Delta) : \Delta \in \mathcal{T}_n\}.$$

We assume there are positive numbers C_μ, C_Δ for which

$$(2.3) \quad R(\Delta) \geq \frac{\delta_n}{C_\mu}$$

$$(2.4) \quad \mu(\Delta) \geq \frac{\delta_n^2}{C_\Delta}$$

for all $\Delta \in \mathcal{T}_n$. These assumptions imply the mesh scheme is uniform over \mathcal{T}_n in the manner with which the elements decrease in size as $n \rightarrow \infty$.

For purposes of numerical integration and interpolation over the triangular elements in \mathcal{T}_n , we need a parameterization of each such triangular element with respect to a standard reference triangle in the plane, namely the unit simplex

$$\sigma = \{(s, t) : 0 \leq s, t, s + t \leq 1\}.$$

Let $\Delta_{n,k} \in \mathcal{T}_n$, and let the vertices of $\Delta_{n,k}$ be denoted by $\{v_1, v_2, v_3\}$. Define a parameterization function $m_k : \sigma \xrightarrow{1-1} \Delta_{n,k}$ by

$$m_k(s, t) = uv_3 + tv_2 + sv_1, \quad (s, t) \in \sigma$$

with $u = 1 - s - t$. Using this, we can write

$$\int_{\Delta_k} f(Q) dS_Q = |D_s m_k \times D_t m_k| \int_{\sigma} f(m_k(s, t)) d\sigma$$

since $|D_s m_k \times D_t m_k|$ is a constant function, equal to twice the area of $\Delta_{n,k}$. This formula can be used to numerically evaluate the left-hand integral by using numerical integration formulas developed for the region σ ; e.g. see [22].

2.1. Interpolatory projections. To define collocation methods, we need to consider interpolation over the surface S . The *centroid* of $\Delta_{n,k}$ is defined as

$$P_k = m_k\left(\frac{1}{3}, \frac{1}{3}\right) = \frac{1}{3}(v_1 + v_2 + v_3).$$

Define the operator \mathcal{P}_n associated with piecewise constant interpolation over S by

$$(\mathcal{P}_n f)(P) = f(P_k), \quad P \in \Delta_k, \quad k = 1, \dots, n$$

for $f \in C(S)$.

We also wish to consider approximations based on piecewise linear approximations over the triangulation \mathcal{T}_n . Given $g \in C(S)$, we define the interpolating function $\mathcal{P}_n g$ as follows, basing it on interpolation over the unit simplex σ . Let α be a given constant with $0 \leq \alpha < \frac{1}{3}$; and define interpolation nodes in σ by

$$(2.5) \quad \{q_1, q_2, q_3\} = \{(\alpha, \alpha), (\alpha, 1 - 2\alpha), (1 - 2\alpha, \alpha)\}.$$

If $\alpha = 0$, these are the three vertices of σ ; and otherwise, they are symmetrically placed points in the interior of σ . Define corresponding *Lagrange interpolation basis functions* by

$$\ell_1(s, t) = \frac{u - \alpha}{1 - 3\alpha}, \quad \ell_2(s, t) = \frac{t - \alpha}{1 - 3\alpha}, \quad \ell_3(s, t) = \frac{s - \alpha}{1 - 3\alpha}$$

for $(s, t) \in \sigma$ and $u = 1 - s - t$. The linear polynomial interpolating $f \in C(\sigma)$ at the nodes of (2.5) is given by

$$f(s, t) \approx \sum_{i=1}^3 f(q_i) \ell_i(s, t).$$

For $g \in C(S)$, define

$$(2.6) \quad (\mathcal{P}_n g)(m_k(s, t)) = \sum_{i=1}^3 g(m_k(q_i)) \ell_i(s, t), \quad (s, t) \in \sigma$$

for $k = 1, 2, \dots, n$. This interpolates $g(P)$ over each triangular element $\Delta_k \subset S$, with the interpolating function linear in the parameterization variables s and t . Let the interpolation nodes in Δ_k be denoted by

$$v_{k,i} = m_k(q_i), \quad i = 1, 2, 3, \quad k = 1, \dots, n.$$

Then (2.6) can be written

$$(2.7) \quad (\mathcal{P}_n g)(P) = \sum_{i=1}^3 g(v_{k,i}) \ell_i(s, t), \quad P = m_k(s, t) \in \Delta_k$$

for $k = 1, \dots, n$. Collectively, we refer to the interpolation nodes $\{v_{k,i}\}$ by $\{v_1, v_2, \dots, v_{3n}\}$, for $\alpha > 0$.

Higher degree extensions can be given of the piecewise constant and piecewise linear interpolation defined above. We refer to [1, Chap. 5] for some of the tools for this, along with results given in [17]. In our experimental studies, we have considered only piecewise constant and piecewise linear interpolation. In the numerical experiments discussed in this paper, we consider collocation methods based on only piecewise linear interpolation. Moreover, we assume

$$0 < \alpha < \frac{1}{3}$$

which forces all interpolation nodes to be interior to each triangle Δ_k .

2.2. Collocation. The collocation method for solving (1.3) or (1.4) can be written abstractly as

$$(2.8) \quad (I - \mathcal{P}_n \mathcal{K})u_n = \mathcal{P}_n E$$

with \mathcal{P}_n an interpolatory projection. Our approximations u_n are generally not continuous over the boundaries of the triangular elements of our mesh for S , in part because our collocation node points are chosen interior to the elements of the triangular mesh \mathcal{T}_n we impose on S . This is done, in part, to avoid having node points on edges of the original surface S as the normal \mathbf{n}_P in (1.2) is undefined where two edges come together. To render the solution graphically with standard software, we would need to know values at the corner points of the triangulation; and that is easily accomplished from the solution we obtain at the interior points, although we do not consider it here.

Let the number of collocation nodes be denoted by d_n ($d_n = n$ for the centroid method, $d_n = 3n$ for the piecewise linear method), and let $\{P_i\}$ denote collectively these nodes. Let

$\{\varphi_i \mid i = 1, \dots, d_n\}$ denote the Lagrange basis functions for the interpolation scheme being used. For the centroid rule,

$$\varphi_i(P) = \begin{cases} 1, & P \in \Delta_i, \\ 0, & P \notin \Delta_i. \end{cases}$$

For piecewise linear interpolation, use the basis functions implicit in (2.7), which are again nonzero over only a single triangular element. We also will write

$$\varphi_{k_j, \ell}(Q), \quad k_{j, \ell} = 3j - 3 + \ell, \quad \ell = 1, 2, 3,$$

for the three linear basis functions over the element Δ_j . Also introduce the parameter $\nu = 1$ for the centroid method, and $\nu = 3$ for the piecewise linear method. These ideas extend naturally to higher degree collocation functions.

The solution of (2.8) reduces to the solution of the linear system

$$(2.9) \quad u_n(P_i) - \frac{\rho(P_i)}{\pi} \sum_{j=1}^n \sum_{\ell=1}^{\nu} u_n(P_{k_j, \ell}) \int_{\Delta_j} V(P_i, Q) G(P_i, Q) \varphi_{k_j, \ell}(Q) dS_Q = E(P_i)$$

with $\{P_{k_j, \ell} : 1 \leq \ell \leq \nu\}$ the ν collocation nodes inside Δ_j , for $i = 1, \dots, d_n$. We denote this system symbolically by

$$(2.10) \quad (I - K_n) \mathbf{u}_n = \mathbf{E}_n,$$

$$(\mathbf{u}_n)_i = u_n(P_i), \quad (\mathbf{E}_n)_i = E(P_i), \quad i = 1, \dots, n.$$

To set up the linear system requires the evaluation of the integrals in (2.9). These may be evaluated either analytically (cf. [20]) or by numerical integration (cf. [6]). Note that for $P, Q \in S_j$ for some j , we have $G(P, Q) = 0$; and this avoids the need to calculate many of the collocation integrals in (2.9). In particular, $(K_n)_{i, i} = 0$ since $G(P_i, Q) \equiv 0$ over a triangular element containing P_i in its interior; and thus the system (2.10) contains no singular integrals, although some are likely to be nearly singular when P_i is near to an edge or corner of S . In addition, if $V(P_i, Q) \equiv 0$ as Q varies over Δ_j , the corresponding integral in (2.9) is zero. For codes evaluating these integrals numerically, see [2] and the discussion in [6].

For more of a computer graphics perspective on the piecewise linear collocation method, and for another way to evaluate analytically the needed collocation integrals, see [7], [8].

2.3. Iteration. A standard iterative method of solution of (2.10) is based on a simple fixed point iteration. Define

$$(2.11) \quad \mathbf{u}_n^{(k+1)} = \mathbf{E}_n + K_n \mathbf{u}_n^{(k)}, \quad k = 0, 1, \dots,$$

for some given initial guess $\mathbf{u}_n^{(0)}$. Easily,

$$\mathbf{u}_n - \mathbf{u}_n^{(k+1)} = K_n \left[\mathbf{u}_n - \mathbf{u}_n^{(k)} \right],$$

and the method converges if $\|K_n\| < 1$. In this case, the matrix norm being used is the row norm, compatible with the maximum norm on \mathbb{R}^{d_n} .

Examining the elements of K_n in the case of piecewise constant interpolation, the elements are all non-negative and for the sum of the i^{th} row, we have

$$\sum_{j=1}^n (K_n)_{i,j} = \frac{\rho(P_i)}{\pi} \int_S V(P_i, Q) G(P_i, Q) dS_Q.$$

It is well-known that

$$\|K_n\| \leq \|\mathcal{K}\|$$

when \mathcal{K} is regarded as an operator on $L^\infty(S)$ to $L^\infty(S)$, and this is known to be bounded away from 1; cf. [6]. This proves the convergence of (2.11), with a rate that is independent of the size of n . For piecewise linear interpolation, we need to further assume that the reflectivity $\rho(P)$ is sufficiently small, although this assumption is probably an artifact of our method of proof.

3. Approximation by clustering. In practical problems d_n can be quite large, too large to set up the system for direct solution by standard Gaussian elimination or standard iteration methods. For larger values of d_n , it is impractical to set up this system completely, and so-called ‘fast matrix-vector multiplication methods’ are needed. An example of such is given in [5] for unoccluded surfaces; and other schemes have been proposed based on the ‘fast multipole method’ and ‘wavelet compression multi-resolution schemes’ (e.g. [11]). For a computer graphics perspective in designing such a fast method, see [13].

There are two main practical problems in dealing with the linear system

$$(3.1) \quad (I - K_n) \mathbf{u}_n = \mathbf{E}_n$$

when n is large. First the setup time for the matrix K_n is proportional to n^2 , with a large constant of proportionality. Second, the cost of the iteration method for solving the system is also proportional to n^2 , even though usually we need only a few iterations. The setup time seems the greater expense in practice, as some of our timings from [5] suggest. In the following we propose a method to reduce the cost of both the matrix setup and the iteration procedure to something less than $O(n^2)$. However, the method will not be as rapid as that given in [5], as we discuss later. The method is based on the work of Hackbusch and Nowak [12], who developed such a method for solving boundary integral equation reformulations of Laplace’s equation in \mathbb{R}^3 . Following we describe their work and adapt it to the radiosity equation. To simplify the presentation and notation, we consider the collocation method with only piecewise constant functions ($\nu = 1$ in (2.9)), but the central ideas are suitable for piecewise polynomial approximations of any fixed degree and our numerical examples use piecewise linear collocation. Based on the results given in [3], it does not seem a worthwhile idea to look at higher degree collocation methods.

We do not compute K_n explicitly. Rather, for a given vector \mathbf{u} , we compute an approximation to $K_n \mathbf{u}$. The cost will be much less than it would be if based on first computing K_n and then following it with the matrix-vector multiplication $K_n \mathbf{u}$, each of which has an operations cost of $O(n^2)$. This approximation of $K_n \mathbf{u}$ is under the control of two parameters m and η to control the approximation error, and the user specifies these parameters. The parameter m is a positive integer and the parameter $\eta \in (0, 1)$; they are introduced below.

Recall

$$(3.2) \quad (K_n \mathbf{u})_i = \sum_{j=1}^n u_j \int_{\Delta_j} K(P_i, Q) dS_Q, \quad i = 1, \dots, n.$$

For each P_i , we subdivide the elements Δ_j of the triangulation \mathcal{T}_n into three distinct subsets, called the *near field*, the *far field*, and the *gray field*.

For each P_i , the gray field for P_i contains those elements Δ_j that contain a ‘visibility line’, meaning that $V(P_i, Q)$ is neither identically 0 nor 1 over Δ_j . The line of discontinuity for $V(P_i, Q)$, as Q varies over Δ_j , is called the *visibility line*. In the original paper [12, §3], there was no need to consider such elements. The larger cost of our adaptation of the clustering method from [12, §3] is due to the existence of this gray field.

The near field contains those elements Δ_j of the triangulation \mathcal{T}_n that are not in the gray field and that are ‘sufficiently close’ to P_i . For elements Δ_j in the near field and the gray field, the corresponding integrals in (3.2) are computed by standard methods; we want to minimize the number of such integrations. The remaining elements in \mathcal{T}_n , those not contained in either the near field or the gray field, are said to make up the *far field*. This separation between the near field and the far field is associated with a parameter η under the user’s control. For Q belonging to an element Δ_j in the far field, we approximate $K(P_i, Q)$ based on a Taylor polynomial of degree $m - 1$ and then we carry out exactly and efficiently all integrations of the Taylor polynomial.

We have a sequence of triangulations $\mathcal{T}_n, n = n_0, n_1, \dots, n_c$ with \mathcal{T}_{n_c} the most current subdivision of S . For simplicity, we assume $n_\ell = 4^\ell n_0, \ell \geq 0$. Let

$$\mathcal{T}_{n_\ell} = \{ \Delta_k^\ell : k = 1, \dots, n_\ell \}, \quad \ell = 0, 1, \dots, c.$$

We refer to this triangulation as being at ‘level ℓ ’. The collection

$$\mathcal{U} = \mathcal{T}_{n_0} \cup \dots \cup \mathcal{T}_{n_c}$$

can be regarded as a tree structure of clusters of the elements from the finest subdivision \mathcal{T}_{n_c} of S , from the various levels of the refinement process. For more on this tree structure and its properties, see [12, §3].

Given a collocation point P_i , we say a cluster $\tau \in \mathcal{U}$ is *admissible* if

$$(3.3) \quad R(\tau) \leq \eta |P_i - A(\tau)|$$

and if $V(P_i, Q)$ is constant as Q varies over τ . If an element $\Delta \in \mathcal{T}_{n_c}$ is not admissible and is not in the gray field of P_i , then we say it is in the *near field* of P_i . The *far field* for P_i is the closure of the complement in S of the union of the near field and gray field for P_i . As η decreases, the size of the near field increases, and this generally increases the cost of approximating $K_n \mathbf{u}$. The size of the gray field is independent of η . For theoretical reasons, we assume there is a constant $\eta_0 \in (0, 1)$ and we consider the parameters η satisfying

$$(3.4) \quad 0 < \eta \leq \eta_0.$$

In the later theoretical analysis of §4, it is shown that if η_0 is chosen sufficiently small, then various estimates will be true for all η satisfying (3.4).

An *admissible covering* of S with respect to P_i is a collection

$$\mathcal{C} = \{ \tau_1, \dots, \tau_q \} \subset \mathcal{U}, \quad S = \bigcup_1^q \tau_i,$$

with each $\tau \in \mathcal{C}$ satisfying

$$\tau \in \mathcal{T}_{n_c} \quad \text{or} \quad \tau \text{ admissible.}$$

It is shown in [12, Prop. 3.9] that for each P_i , there is a unique minimal admissible covering, unique in the sense of containing a minimum number of clusters τ .

To evaluate $(K_n \mathbf{u})_i$, begin by writing the unique minimal admissible covering of S with respect to P_i by

$$S = \left[\Delta_{i_1}^c \cup \cdots \cup \Delta_{i_q}^c \right] \cup [\tau_1 \cup \cdots \cup \tau_p]$$

with each τ_i an admissible cluster and each $\Delta_{i_j}^c$ a non-admissible element of the current triangulation \mathcal{T}_{n_c} (meaning $\Delta_{i_j}^c$ belongs to either the near field or the gray field of P_i). Then

$$(3.5) \quad (K_n \mathbf{u})_i = \sum_{j=1}^q u_{i_j} \int_{\Delta_{i_j}^c} K(P_i, Q) dS_Q + \sum_{j=1}^p \int_{\tau_j} u_n(Q) K(P_i, Q) dS_Q.$$

The function $u_n(Q)$ is the piecewise constant function over \mathcal{T}_{n_c} with values determined from \mathbf{u} . The first integrals (over the near field and gray field) are evaluated by traditional means, by analytic or numerical integration, and this is discussed at greater length in [6], [20]. For a gray field integral over an element $\Delta \in \mathcal{T}_{n_c}$, it is important to determine accurately the location of the visibility line that intersects Δ , thus allowing an accurate numerical or exact integral to be computed. For the the remaining integrals over the far field, we proceed as follows.

3.1. The far field integration. For the integral over τ_j in (3.5), we use Taylor polynomial approximations of $G(P_i, Q)$ and then perform the remaining integration exactly. We now explain how to do this with some efficiency. This follows ideas in [12].

Let $\tau \in \mathcal{U}$. Using a Taylor approximation in Q of degree $m - 1$ about $A(\tau)$, write

$$(3.6) \quad \frac{[(Q - P) \cdot \mathbf{n}_P]}{|P - Q|^4} \approx \sum_{\alpha \in I_m} a_\alpha(P) (Q - A(\tau))^\alpha, \quad Q \in \tau$$

with $A(\tau)$ the center of the circumscribing circle for τ , as introduced earlier. The set I_m consists of all multi-integers $\alpha = (\alpha_1, \alpha_2, \alpha_3)$ with

$$\alpha_1, \alpha_2, \alpha_3 \geq 0, \quad \alpha_1 + \alpha_2 + \alpha_3 < m.$$

As customary, if $Q = (\xi, \eta, \zeta)$, then $Q^\alpha = \xi^{\alpha_1} \eta^{\alpha_2} \zeta^{\alpha_3}$. We often refer to m as the *order* of the Taylor polynomial approximation.

From (3.6), we can obtain an analogous approximation of $G(P, Q)$:

$$(3.7) \quad \frac{[(Q - P) \cdot \mathbf{n}_P] [(P - Q) \cdot \mathbf{n}_Q]}{|P - Q|^4} \approx \sum_{\alpha \in I_m} b_\alpha(P) (Q - A(\tau))^\alpha.$$

Note that \mathbf{n}_Q is constant over any $\tau \in \mathcal{U}$. More important in obtaining (3.7) from (3.6), the quantity $(P - Q) \cdot \mathbf{n}_Q$ is constant over an element τ . To see this, decompose $P - Q$ into components perpendicular and parallel to τ . All variation in $P - Q$ takes place parallel to τ as Q varies over τ , and the part perpendicular to τ remains constant. Forming the dot product with \mathbf{n}_Q , the portion parallel to τ is zero, and the result follows that $(P - Q) \cdot \mathbf{n}_Q$ is constant over τ .

Next, expand and rearrange the terms in (3.7) into the form

$$(3.8) \quad G(P, Q) \approx \sum_{\alpha \in I_m} \kappa_\alpha(P, A(\tau)) Q^\alpha, \quad Q \in \tau.$$

Return to (3.5), to the approximation of

$$\int_{\tau_j} u_n(Q) G(P_i, Q) dS_Q.$$

Recalling that $V(P_i, Q) \equiv 1$ for Q in a far field element, use (3.8) to write

$$\int_{\tau_j} u_n(Q) K(P_i, Q) dS_Q \approx \frac{\rho(P_i)}{\pi} \sum_{\alpha \in I_m} \kappa_\alpha(P, A(\tau)) \int_{\tau_j} u_n(Q) Q^\alpha dS_Q.$$

The integrals

$$(3.9) \quad \int_{\tau} u_n(Q) Q^\alpha dS_Q, \quad \tau \in \mathcal{U}, \quad \alpha \in I_m$$

can be evaluated explicitly, and they can be obtained in a preprocessing step before beginning the iterative solution of (3.1).

What is the operations cost of calculating these integrals? The cost of producing (3.9) is independent of P and of the center of expansion $A(\tau)$, and thus these integrals can be obtained in $O(n)$ steps. For unoccluded surfaces S , this will result in there being only $O(n)$ such integrals to be evaluated.

In greater detail, let $\tau \in \mathcal{U}$. Then we can write

$$\tau = \Delta_{i_1}^c \cup \cdots \cup \Delta_{i_k}^c$$

for some elements $\Delta_{i_j}^c \in \mathcal{T}_{n_c}$. Then

$$(3.10) \quad \int_{\tau} u_n(Q) Q^\alpha dS_Q = \sum_{j=1}^k u_n(Q) \int_{\Delta_{i_j}^c} Q^\alpha dS_Q$$

since $u_n(Q)$ is constant over each element in \mathcal{T}_{n_c} . Produce the integrals over the elements of \mathcal{T}_{n_c} , and then extend those to the remaining clusters $\tau \in \mathcal{U}$ using (3.10). Since we are working with S a polyhedral surface, the integrals on the right side of (3.10) can be evaluated explicitly. Again the cost is $O(n)$ operations.

Following Hackbusch and Nowak [12], it can be shown that with appropriate choices of $\eta = \eta(n)$ and $m = m(n)$, the quantity $K_n \mathbf{u}_n$ can be approximated, say by $\widetilde{K}_n \mathbf{u}_n$ with

$$(3.11) \quad \left\| K_n \mathbf{u}_n - \widetilde{K}_n \mathbf{u}_n \right\|_{\infty} = O(h^\kappa) \|\mathbf{u}_n\|_{\infty}, \quad \mathbf{u}_n \in \mathbb{R}^{d_n}$$

with κ the order of the underlying numerical scheme being used. If we assumed sufficient regularity in the unknown solution u , then κ is the order of the collocation approximation method being used. For piecewise constant collocation, $\kappa = 1$ and for piecewise linear collocation, $\kappa = 2$. The derivation of (3.11) is discussed in detail in §4.1. The result (3.11) also assumes the near field integrals in (3.5) are evaluated with an error consistent with the right side; in some cases they can be evaluated exactly. For notational purposes, we write

$$\widetilde{K}_n \mathbf{u}_n = \widetilde{K}_n \widetilde{\mathbf{u}}_n$$

with \widetilde{K}_n a square matrix of order d_n . We never produce this matrix \widetilde{K}_n explicitly, but it is useful when giving a theoretical analysis of the approximation.

The cost of evaluating the portion of $\widetilde{K}_n \mathbf{u}_n$ associated with the far field is shown in [12] to be $O(n \log^5 n)$ operations. Unfortunately, we have the additional cost of evaluating the collocation integrals in (2.9) for the elements Δ_j in the gray field for P_i . With a uniform triangulation of S , as assumed in (2.3)-(2.4), even a single visibility line for a field point P_i cutting across a face of S will lead to $O(\sqrt{n})$ elements intersected by such a line and thus to an additional operations cost of $O(\sqrt{n})$. When looking at the cumulative effect of $O(n)$ such points P_i , we have an additional operations cost of size

$$(3.12) \quad O(n\sqrt{n}).$$

Thus the total operations cost cannot be brought below $O(n\sqrt{n})$ for most occluded surfaces of practical interest, even when we retain the efficiency of the approximations in [12] for the near and far fields. This result is an improvement on the cost of $O(n^2)$ for the standard setup and iterative solution, but not what we would have liked.

The near-optimal performance of the clustering method in [12] cannot be matched when applied to the radiosity equation. Moreover, we do not see how any fast matrix-vector multiplication method can avoid this problem, due to the $O(\sqrt{n})$ elements intersected by each visibility line for $O(n)$ collocation points.

4. Theoretical error analysis . In this section, we discuss the error caused by the approximation of the far field integrations. The numerical integration of integrals over elements in the near field and the gray field is discussed at greater length in [6].

As we mentioned in §2.2, the collocation method for solving (1.3) or (1.4) can be written abstractly as (2.8),

$$(I - \mathcal{P}_n \mathcal{K}) \mathbf{u}_n = \mathcal{P}_n E$$

The solution of this equation reduces to the solution of the linear system (2.9), or symbolically as in (2.10),

$$(I - K_n) \mathbf{u}_n = \mathbf{E}_n.$$

K_n is then approximated by \widetilde{K}_n using the method described in §3.1. Instead of solving the above system, we solve the system

$$(4.1) \quad (I - \widetilde{K}_n) \widetilde{\mathbf{u}}_n = \mathbf{E}_n.$$

Using standard perturbation theory, we can guarantee the unique solvability of this new approximation for n chosen sufficiently large.

From the theoretical error analysis for the original collocation method, it is known that $(I - K_n)^{-1}$ exists and is uniformly bounded for all sufficiently large n , say for $n \geq N$. In addition, if u is sufficiently smooth, then

$$(4.2) \quad \|\mathbf{u} - \mathbf{u}_n\|_\infty = O(h^\kappa), \quad n \geq N$$

with κ defined following (3.11); cf. [6]. From (3.11) (or from Theorem 4.1 given below) we have that $\|K_n - \widetilde{K}_n\|$ is sufficiently small for all large values of n . Using standard perturbation theory, we have that $(I - \widetilde{K}_n)^{-1}$ also exists and is uniformly bounded in n . Then the system in (4.1) is uniquely solvable for all large values of n .

Write

$$\mathbf{u} - \widetilde{\mathbf{u}}_n = (\mathbf{u} - \mathbf{u}_n) + (\mathbf{u}_n - \widetilde{\mathbf{u}}_n)$$

$$\|\mathbf{u} - \tilde{\mathbf{u}}_n\|_\infty \leq \|\mathbf{u} - \mathbf{u}_n\|_\infty + \|\mathbf{u}_n - \tilde{\mathbf{u}}_n\|_\infty.$$

Using the identity

$$(4.3) \quad \mathbf{u}_n - \tilde{\mathbf{u}}_n = (I - \tilde{K}_n)^{-1}(K_n - \tilde{K}_n)\mathbf{u}_n$$

we have

$$\|\mathbf{u}_n - \tilde{\mathbf{u}}_n\|_\infty \leq \|(I - \tilde{K}_n)^{-1}\| \cdot \|(K_n - \tilde{K}_n)\mathbf{u}_n\|.$$

When combined with (3.11) and (4.2), we have

$$\|\mathbf{u} - \tilde{\mathbf{u}}_n\|_\infty = O(h^\kappa), \quad n \geq N.$$

We note an implicit assumption to this work and to that of Hackbusch and Nowak [12]. We want to choose the approximation \tilde{K}_n in such a way that the operations count for calculating $\tilde{K}_n \mathbf{u}_n$ is minimized while simultaneously maintaining the rate of convergence of the original collocation solution in (4.2). This is the reason for desiring the result (3.11), as it leads via (4.3) to the desired rate of convergence and to the operation counts that we obtain. In contrast, many fast methods used in the computer graphics community ask only that the error $K_n \mathbf{u}_n - \tilde{K}_n \mathbf{u}_n$ be smaller than something related to the pixel size of the display device; e.g., see [13]. Both of these perspectives are reasonable, but they can lead to markedly different interpretations of the phrase ‘optimal operation counts’.

4.1. The error in clustering. We follow the development in [12] to bound

$$\|(K_n - \tilde{K}_n)\mathbf{u}_n\|$$

and to bound the numbers of elements in the near and far fields of the triangulation. We do so in the context of all our sub-surfaces being polygonal and planar, and of \mathcal{K} being the radiosity integral operator. In this case, more precise results can be obtained and some steps in the proof are simplified. As notation, recall the definition of δ_n in (2.2) and let $\delta \equiv \delta_{n_c}$, with n_c the index for the current finest level mesh \mathcal{T}_{n_c} .

THEOREM 4.1. *Let m be the order of the Taylor expansion of the kernel. Let K_n and \tilde{K}_n be described as above. Then*

$$(4.4) \quad \|(K_n - \tilde{K}_n)\mathbf{u}_n\| \leq C_{m-1}(2\eta)^m \|\mathbf{u}_n\|_\infty \frac{\mu(S)\eta_0^2 C_\mu^2}{\delta^2(1 + \eta_0^2)}$$

where

$$C_{m-1} = \frac{(1 + \eta_0)^4 2^3}{(1 - \eta_0)^{m+4}}.$$

Proof. Define

$$k(x, y) = \frac{(\mathbf{y} - \mathbf{x}) \cdot \mathbf{n}_x}{|\mathbf{x} - \mathbf{y}|^4},$$

where x , y , and n_x are vectors in \mathbb{R}^3 . Let $k_{m-1}(x, y)$ be its Taylor expansion of degree $m - 1$ around $y_0 \in \mathbb{R}^3$. There exists $t \in (0, 1)$ such that the remainder

$$\begin{aligned} & R_{m-1}(x - y_0, y - y_0) \\ &= k(x, y) - k_{m-1}(x, y) = \frac{1}{m!} \left(\frac{d}{dt} \right)^m \frac{(\mathbf{y}_0 + t(\mathbf{y} - \mathbf{y}_0) - \mathbf{x}) \cdot \mathbf{n}_x}{|(\mathbf{x} - \mathbf{y}_0) - t(\mathbf{y} - \mathbf{y}_0)|^4} \\ &= \frac{1}{m!} \left(\frac{d}{dt} \right)^m \frac{-((\mathbf{x} - \mathbf{y}_0) - t(\mathbf{y} - \mathbf{y}_0)) \cdot \mathbf{n}_x}{|(\mathbf{x} - \mathbf{y}_0) - t(\mathbf{y} - \mathbf{y}_0)|^4}. \end{aligned}$$

Define

$$\phi(t) = \frac{-(\xi - t\zeta) \cdot n_x}{|\xi - t\zeta|^4}, \quad t \in \mathbb{R}, \quad \xi, \zeta, n_x \in \mathbb{R}^3.$$

The analytic continuation

$$\phi(z) = \frac{-(\xi - z\zeta) \cdot n_x}{|\xi - z\zeta|^4}$$

is holomorphic in $|z| < 1/\alpha$ with

$$\alpha = \alpha(\xi, \zeta) = \frac{|\zeta|}{|\xi|} \leq \eta_0 < 1.$$

Cauchy's integral formula yields

$$\frac{1}{m!} \phi^{(m)}(t) = \frac{1}{2\pi i} \oint_{|z|=r} \frac{\phi(z) dz}{(z-t)^{m+1}} \quad \text{for } |t| < r < \frac{1}{\alpha}.$$

Since

$$\begin{aligned} |\phi(z)| &= \frac{|(\xi - z\zeta) \cdot n_x|}{|\xi - z\zeta|^4} \leq \frac{|\xi - z\zeta| |n_x| \cos \theta}{|\xi - z\zeta|^4} \leq \frac{1}{|\xi - z\zeta|^3} \leq \frac{1}{\left| |\xi| - |z| |\zeta| \right|^3} \\ &= \frac{1}{|\xi|^3 \left| 1 - r \frac{|\zeta|}{|\xi|} \right|^3} = \frac{1}{|\xi|^3 |1 - r\alpha|^3} \quad \text{for } |z| = r \end{aligned}$$

and

$$|z - t| \geq r - 1$$

for $0 < t < 1 < r = |z|$, we have

$$\begin{aligned} \left| \frac{1}{m!} \phi^{(m)}(t) \right| &= \left| \frac{1}{2\pi i} \oint_{|z|=r} \frac{\phi(z) dz}{(z-t)^{m+1}} \right| \leq \frac{1}{2\pi} \oint_{|z|=r} \frac{|\phi(z)| d|z|}{|z-t|^{m+1}} \\ &\leq \frac{1}{2\pi} \frac{1}{|\xi|^3 |1 - r\alpha|^3} \frac{2\pi r}{(r-1)^{m+1}} = \frac{r}{|\xi|^3 |1 - r\alpha|^3 (r-1)^{m+1}}. \end{aligned}$$

For

$$r = \frac{1}{2} \left(1 + \frac{1}{\alpha} \right) = \frac{\alpha + 1}{2\alpha} \in \left(1, \frac{1}{\alpha} \right),$$

the above equation becomes

$$\begin{aligned} \left| \frac{1}{m!} \phi^{(m)}(t) \right| &\leq \frac{(\alpha + 1)}{2\alpha |\xi|^3} \left| 1 - \frac{\alpha + 1}{2} \right|^{-3} \left(\frac{2\alpha}{1 - \alpha} \right)^{m+1} \\ &= \left(\frac{\alpha + 1}{1 - \alpha} \right) \frac{1}{|\xi|^3} \left(\frac{2}{1 - \alpha} \right)^3 \left(\frac{2\alpha}{1 - \alpha} \right)^m \\ &\leq \left(\frac{1 + \eta_0}{1 - \eta_0} \right) \frac{1}{|\xi|^3} \left(\frac{2}{1 - \eta_0} \right)^3 \left(\frac{2\alpha}{1 - \eta_0} \right)^m = \left(\frac{1 + \eta_0}{1 - \eta_0} \right) \left(\frac{2}{1 - \eta_0} \right)^{m+3} \frac{\alpha^m}{|\xi|^3}. \end{aligned}$$

The estimate

$$\frac{|\xi - \zeta|}{|\xi|} = \left| \frac{\xi}{|\xi|} - \frac{\zeta}{|\xi|} \right| \leq \left| 1 - \frac{|\zeta|}{|\xi|} \right| \leq 1 + \alpha \leq 1 + \eta_0$$

implies that

$$\frac{1}{|\xi|} \leq \frac{1 + \eta_0}{|\xi - \zeta|}.$$

Thus,

$$\begin{aligned} |R_{m-1}(\xi, \zeta)| &= \left| \frac{1}{m!} \phi^{(m)}(t) \right| \leq \left(\frac{1 + \eta_0}{1 - \eta_0} \right) \left(\frac{2}{1 - \eta_0} \right)^{m+3} |\xi|^{-3} \alpha^m \\ (4.5) \quad &\leq \left(\frac{1 + \eta_0}{1 - \eta_0} \right) \left(\frac{2}{1 - \eta_0} \right)^{m+3} \alpha^m \left(\frac{1 + \eta_0}{|\xi - \zeta|} \right)^3. \end{aligned}$$

For $\xi = x - y_0$, $\zeta = y - y_0$, $\xi - \zeta = x - y$, with $|y - y_0| \leq \eta|x - y_0|$, where

$$\eta \leq \eta_0,$$

and define

$$\bar{\eta} = \frac{\eta}{\sqrt{1 + \eta^2}}.$$

Now, (4.5) becomes

$$\begin{aligned} |k(x, y) - k_{m-1}(x, y)| &= |R_{m-1}(x - y_0, y - y_0)| \\ &\leq \left(\frac{1 + \eta_0}{1 - \eta_0} \right) \left(\frac{2}{1 - \eta_0} \right)^{m+3} \alpha^m \left(\frac{1 + \eta_0}{|\xi - \zeta|} \right)^3 \\ &= \left(\frac{1 + \eta_0}{1 - \eta_0} \right) \left(\frac{2}{1 - \eta_0} \right)^{m+3} \left(\frac{|y - y_0|}{|x - y_0|} \right)^m \left(\frac{1 + \eta_0}{|(x - y_0) - (y - y_0)|} \right)^3 \\ &\leq \left(\frac{1 + \eta_0}{1 - \eta_0} \right) \left(\frac{2}{1 - \eta_0} \right)^{m+3} \eta^m \left(\frac{1 + \eta_0}{|x - y|} \right)^3 = \frac{(1 + \eta_0)^4 2^3 (2\eta)^m}{(1 - \eta_0)^{m+4} |x - y|^3} \\ &= C_{m-1} (2\eta)^m |x - y|^{-3}. \end{aligned}$$

For the radiosity kernel,

$$k(P, Q) = \frac{[(Q - P) \cdot \mathbf{n}_P][(P - Q) \cdot \mathbf{n}_Q]}{|P - Q|^4}.$$

Let k_{m-1} be the Taylor expansion of degree $m - 1$ about Q_0 for

$$\frac{[(Q - P) \cdot \mathbf{n}_P]}{|P - Q|^4}.$$

The error is

$$\begin{aligned} |k(P, Q) - k_{m-1}(P, Q)| &= |[(P - Q) \cdot \mathbf{n}_Q]| \left| \frac{[(Q - P) \cdot \mathbf{n}_P]}{|P - Q|^4} - k_{m-1}(P, Q) \right| \\ &\leq |P - Q| \frac{C_{m-1} (2\eta)^m}{|P - Q|^3} \leq \frac{C_{m-1} (2\eta)^m}{|P - Q|^2}. \end{aligned}$$

Given any point $P \in S$. $\mathcal{C}(P)$ is an admissible covering of S w.r.t. P . Let

$$F(P) = \bigcup \{ \tau \in \mathcal{C}(P) : \tau \text{ is admissible with respect to } P \}.$$

For every $\tau \in F(P)$, $R(\tau) \leq \bar{\eta} \cdot \text{dist}(P, \tau)$, which implies

$$\text{dist}(P, \tau) \geq R(\tau)/\bar{\eta}.$$

For every $\tau \notin F(P)$, $R(\tau) > \bar{\eta} \cdot \text{dist}(P, \tau)$, which implies

$$\text{dist}(P, \tau) < R(\tau)/\bar{\eta}.$$

Note, $\tau \notin F(P)$ means that τ is a panel in near field. For every $\tau \in F(P)$, τ is either a panel in \mathcal{T}_{n_e} or a cluster which contains several panels. Therefore,

$$R(\tau) \geq R(\Delta) > \frac{\delta}{C_\mu} \quad \text{for some } \Delta \in \mathcal{T}_{n_e}.$$

For every $\tau \in F(P)$,

$$\text{dist}(P, \tau) \geq \frac{R(\tau)}{\bar{\eta}} > \frac{\delta}{C_\mu \bar{\eta}}.$$

Thus,

$$F(P) \subset S \setminus K_r(P)$$

where

$$K_r(P) = \{Q \mid |P - Q| \leq r\}$$

and

$$r = \frac{\delta}{C_\mu \bar{\eta}}.$$

Since $x/\sqrt{1+x^2}$ is increasing for $x \in [0, 1]$,

$$\bar{\eta} = \frac{\eta}{\sqrt{1+\eta^2}} \leq \frac{\eta_0}{\sqrt{1+\eta_0^2}}.$$

Then,

$$r = \frac{\delta}{C_\mu \bar{\eta}} = \frac{\delta}{C_\mu \frac{\eta}{\sqrt{1+\eta^2}}} \geq \frac{\delta}{C_\mu \frac{\eta_0}{\sqrt{1+\eta_0^2}}} = \delta \frac{\sqrt{1+\eta_0^2}}{\eta_0 C_\mu} = C_S \delta$$

where

$$C_S = \frac{\sqrt{1+\eta_0^2}}{\eta_0 C_\mu}.$$

The additional error caused by the Taylor expansion of the kernel is

$$\begin{aligned}
 & \left| K \mathbf{u}_n(P) - \tilde{K} \mathbf{u}_n(P) \right| \\
 & \leq \left| \int_{F(P)} (k(P, Q) - k_{m-1}(P, Q)) \mathbf{u}_n(P) dS_Q \right| \\
 & \leq C_{m-1} (2\eta)^m \|\mathbf{u}_n\|_\infty \int_{S \setminus K_{C_S \delta}} \frac{dS_Q}{|P - Q|^2} \\
 & \leq C_{m-1} (2\eta)^m \|\mathbf{u}_n\|_\infty \int_{S \setminus K_{C_S \delta}} \frac{\eta_0^2 C_\mu^2 dS_Q}{\delta^2 (1 + \eta_0^2)} \\
 & = C_{m-1} (2\eta)^m \|\mathbf{u}_n\|_\infty \frac{\mu(S) \eta_0^2 C_\mu^2}{\delta^2 (1 + \eta_0^2)}.
 \end{aligned}$$

Thus the proof is completed. \square

4.2. The number of clusters. We give an estimation of the number $\sigma(x)$ of clusters in the minimum admissible covering $\mathcal{C}(x)$ with respect to x and the number of non-admissible triangles in $\mathcal{C}(x)$.

Recall the definitions of δ and C_μ in (2.2) and (2.3), respectively. Since S is the union of planes,

$$(4.6) \quad \mu(K_r(z) \cap S) \leq \pi r^2 \quad \text{for all } r \geq 0, z \in \mathbb{R}^3.$$

We begin with the following lemma.

LEMMA 4.2. *The condition (4.6) implies*

$$(4.7) \quad n\delta^2 \geq \frac{\mu(S)}{\pi} > 0$$

and

$$\mu(\Delta) \leq \pi R(\Delta)^2 \text{ for all } \Delta \in \mathcal{T}_{n_c}.$$

Proof. Since $\Delta \subset K_{R(\Delta)}(A(\Delta)) \cap S$,

$$\mu(\Delta) \leq \mu(K_{R(\Delta)}(A(\Delta)) \cap S) \leq \pi R(\Delta)^2.$$

Then,

$$\mu(S) = \sum_{\Delta \in \mathcal{T}_{n_c}} \mu(\Delta) \leq \pi \sum_{\Delta \in \mathcal{T}_{n_c}} R(\Delta)^2 \leq \pi \sum_{\Delta \in \mathcal{T}_{n_c}} \delta^2 = \pi n \delta^2.$$

\square

Before we prove the next theorem, we assume the following condition. This condition describes how a limited part of S is covered by a part \mathcal{C}' of an admissible covering. An upper bound of number of elements in \mathcal{C}' is given by (4.9), provided the clusters in the admissible covering all have the size $R(\tau) \leq r$.

CONDITION 4.3. *For any point $z \in S$ and $R \geq r > 0$ there is an admissible covering with respect to z for which there exists a subset $\mathcal{C}' \subset \mathcal{U}$ with*

$$(4.8) \quad \begin{aligned} & S \cap \overline{K_R(z)} \subset \cup \{\tau \in \mathcal{C}'\} \\ & R(\tau) \leq r \quad \text{for all } \tau \in \mathcal{C}' \setminus \mathcal{T}_{n_c} \end{aligned}$$

$$(4.9) \quad \#\mathcal{C}' \leq 2(R/r)^2.$$

THEOREM 4.4. *Let n be the number of elements and η be the ratio. The number $\sigma(x)$ of cluster in the minimum admissible covering $\mathcal{C}(x)$ w.r.t. x is bounded by the following inequality:*

$$(4.10) \quad \sigma(x) \leq C_\sigma \left(\frac{1}{\eta}\right)^2 \log(2 + \eta^2 n) \quad \text{for all } x \in S.$$

Proof. Let the size of $S \in \mathcal{U}$ is $\rho = R(S)$. First we assume that

$$|x - A(S)| \leq \rho \text{ implying } S \subset \overline{K_R(x)} \text{ for } R = 2\rho.$$

In later step, we consider the case of $|x - A(S)| > \rho$.

In this step, we calculate how many clusters each annulus contains. For all $l = 0, 1, \dots$, we apply the condition (4.3) with $z = x$, $R = R_l = 2^{1-l}\rho$, and

$$r = r_l = \frac{R_l \bar{\eta}}{4}.$$

There are coverings \mathcal{C}_l with

$$\begin{aligned} S \cap \overline{K_R(x)} &\subset \cup \{\tau^l \in \mathcal{C}_l\}, \\ \#\mathcal{C}_l &\leq 2 \left(\frac{R_l}{r_l}\right)^2 = 2 \left(\frac{R_l}{R_l \bar{\eta}/4}\right)^2 = 2 \left(\frac{4}{\bar{\eta}}\right)^2, \quad l = 0, 1, \dots \end{aligned}$$

Let

$$K^l = \overline{K_{R_l}(x)} \setminus K_{R_l/2}(x)$$

and define $\mathcal{C}'_l \subset \mathcal{C}_l$ by

$$\mathcal{C}'_l = \{\tau^l \in \mathcal{C}_l : \tau \cap K^l \neq \emptyset\}.$$

Note that K^l is an annulus, and \mathcal{C}'_l contains clusters which covers K^l . If $\tau \in \mathcal{C}'_l$ is not a panel, it satisfies

$$R(\tau) \leq r_l = \frac{R_l \bar{\eta}}{4},$$

by (4.8). Since $|y - x| \geq R_l/2$ for any $y \in \tau \cap K^l \neq \emptyset$,

$$\begin{aligned} \text{dist}(x, \tau) &= \inf_{\xi \in \tau} |x - \xi| \geq \inf_{\xi \in \tau} \{|x - y| - |y - \xi|\} \geq \frac{R_l}{2} - r_l = \frac{R_l}{2} - \frac{R_l \bar{\eta}}{4} \\ &> \frac{R_l}{2} - \frac{R_l}{4} = \frac{R_l}{4} = \frac{r_l}{\bar{\eta}} \geq \frac{R(\tau)}{\bar{\eta}}. \end{aligned}$$

Thus, $R(\tau) \leq \bar{\eta} \cdot \text{dist}(x, \tau)$. We can conclude that τ is admissible w.r.t. x for any $\tau \in \mathcal{C}'_l$. Hence, \mathcal{C}'_l is an admissible covering of $K^l \cap S$ w.r.t. x . We have

$$(K^l \cap S) \subset (\cup \{\tau \in \mathcal{C}'_l\})$$

and $\tau \in (\mathcal{C}'_l \setminus \mathcal{T}_{n_c})$ is admissible w.r.t. x . The number of elements in the set \mathcal{C}'_l is

$$\#\mathcal{C}'_l \leq \#\mathcal{C}_l \leq 2 \left(\frac{4}{\bar{\eta}}\right)^2.$$

Let $L \geq 0$ be the first integer with

$$r_L = \frac{R_L \bar{\eta}}{4} = \frac{2^{1-L} \rho \bar{\eta}}{4} \leq \frac{\delta}{C_\mu}.$$

(δ/C_μ is fixed from (2.3) and r_l 's are getting smaller when l 's are getting larger.) Then no $\tau \in \mathcal{C}_L$ can satisfy $R(\tau) \leq r_L$; hence by (4.8), all $\tau \in \mathcal{C}_L$ are panels, i.e., $\mathcal{C}_L \subset \mathcal{T}_{n_c}$. Let

$$\mathcal{C}' = \mathcal{C}'_0 \cup \mathcal{C}'_1 \cup \cdots \cup \mathcal{C}'_{L-1} \cup \mathcal{C}_L.$$

Since the clusters of \mathcal{C}' are not disjoint, we restrict \mathcal{C}' to

$$\mathcal{C} = \{\tau' \in \mathcal{C}' \mid \text{there is no } \tau \in \mathcal{C}' \text{ with } \tau' \subsetneq \tau\}.$$

\mathcal{C} satisfies

$$\begin{aligned} \bigcup \{\tau \in \mathcal{C}\} &= \bigcup \{\tau \in \mathcal{C}'\} \\ &= \bigcup_{l=0}^{L-1} (\cup \{\tau \in \mathcal{C}'_l\}) \cup (\cup \{\tau \in \mathcal{C}_L\}) \supset S \cap \left[\bigcup_{l=0}^{L-1} K^l \cup K_{2^{1-L}\rho}(x) \right] \\ &= S \cap \overline{K_{R_0}(x)} = S. \end{aligned}$$

Thus, \mathcal{C} is a covering of S . If $\tau \in \mathcal{C}$, then $\tau \in \mathcal{C}'_l$ for some $l < L$ or $\tau \in \mathcal{C}_L$. In the former case τ is admissible. In the latter case $\tau \in \mathcal{T}_{n_c}$ holds. Therefore, all $\tau \in \mathcal{C} \setminus \mathcal{T}_{n_c}$ are admissible w.r.t. x . The number of clusters in \mathcal{C} is estimated in

$$\begin{aligned} \#\mathcal{C} &\leq \#\mathcal{C}' \leq \sum_{l=0}^{L-1} \#\mathcal{C}'_l + \#\mathcal{C}_L \leq \sum_{l=0}^{L-1} \#\mathcal{C}_l \leq \sum_{l=0}^{L-1} 2 \left(\frac{4}{\bar{\eta}} \right)^2 \\ &= (L+1)2 \left(\frac{4}{\bar{\eta}} \right)^2 \leq C \left(\frac{1}{\bar{\eta}} \right)^2. \end{aligned}$$

L is the first integer such that the following relation is true,

$$\frac{2^{1-L} \rho \bar{\eta}}{4} \leq \frac{\delta}{C_\mu} \implies 2^{-L} \leq \frac{2\delta}{\rho \bar{\eta} C_\mu} \implies L \geq \log_2 \left(\frac{\rho C_\mu \bar{\eta}}{2\delta} \right).$$

Then

$$\begin{aligned} L &\leq \log_2 \left(\frac{\rho C_\mu \bar{\eta}}{\delta} \right) \leq \log_2 \left(\frac{\rho C_\mu \bar{\eta} \pi^{\frac{1}{2}} n^{\frac{1}{2}}}{(\mu(S))^{\frac{1}{2}}} \right) \quad (\text{Use (4.7)}) \\ &= \log_2 \left(\frac{\rho C_\mu \pi^{\frac{1}{2}}}{(\mu(S))^{\frac{1}{2}}} \right) + \log_2 \left(\bar{\eta} n^{\frac{1}{2}} \right) = O(\log(2 + \eta^2 n)). \end{aligned}$$

Now we proof the case of $|x - A(S)| > \rho$. Let

$$\hat{x} = z_S + \rho \frac{x - A(S)}{|x - A(S)|}.$$

Note that $|\hat{x} - A(S)| \leq \rho$. Let \mathcal{C} be the admissible covering w.r.t. \hat{x} as constructed before. Since $\text{dist}(x, \tau) \geq \text{dist}(\hat{x}, \tau)$ for all $\tau \in \mathcal{U}$, is also admissible w.r.t. x . Thus, the estimate (4.10) is true for all $x \in S$. \square

THEOREM 4.5. *Let n be the number of panel and η be the ratio. Assume (4.6). The number $\sigma'(x)$ of non-admissible panels in $\mathcal{C}(x)$ is bounded by the inequality:*

$$(4.11) \quad \sigma'(x) \leq C_{\sigma'} \left(\frac{1}{\eta} \right)^2 \quad \text{for all } x \in S.$$

Proof. Proposition 3.9(b) of [12] states that all admissible coverings w.r.t. x have the same number $\sigma'(x)$ of non-admissible panels. Let $\mathcal{C}(x)$ be \mathcal{T}_{n_c} . Then, $\mathcal{C}(x)$ has $\sigma'(x)$ non-admissible panels w.r.t. x .

Let $r = 2\delta/\eta$. For any $\Delta \in \mathcal{T}_{n_c}$ and $\Delta \not\subset K_r(x)$, it is admissible w.r.t. x . This is because that

$$|x - A(\Delta)| \geq r - \delta$$

for $\Delta \not\subset K_r(x)$ and δ is defined in (2.2). Now,

$$\eta|x - A(\Delta)| \geq \eta(r - \delta) = 2\delta - \eta\delta \geq \delta \geq R(\Delta).$$

Thus, such Δ is admissible by (3.3). Therefore, $\sigma'(x) \leq \#\mathcal{C}'$ where

$$\mathcal{C}' = \{\Delta \in \mathcal{T}_{n_c} \mid \Delta \subset K_r(x)\}.$$

With (4.6) and (2.4), we have

$$\sigma'(x) \cdot \frac{\delta^2}{C_\Delta} \leq \sum_{\Delta \in \mathcal{C}'} \mu(\Delta) = \mu(\cup\{\pi \in \mathcal{C}'\}) \leq \mu(K_r(x) \cap S) \leq \pi r^2.$$

Thus,

$$\sigma'(x) \leq \frac{\pi r^2 C_\Delta}{\delta^2} = \frac{\pi C_\Delta}{\delta^2} \cdot \left(\frac{2\delta}{\eta}\right)^2 = C_{\sigma'} \left(\frac{1}{\eta}\right)^2$$

where

$$C_{\sigma'} = 4\pi C_\Delta.$$

□

5. The experimental problems. For S , we use the following 5-piece surface. It consists of four squares and one rectangular piece, labeled as S_1, S_2, S_3, S_4, S_5 . In particular,

- $S_1 = [0, A] \times [0, A]$ in the xy -plane, facing upward;
- S_2 and S_3 are the bottom and top, respectively, of $[0, B] \times [0, B]$ in the plane $z = 1$;
- $S_4 = [0, C] \times [0, C]$ in the plane $z = 2$, facing downward;
- $S_5 = \{(x, A, z) : 0 \leq x \leq A, 0 \leq z \leq 1\}$, using the side that is visible from S_1, S_2 , and S_4 .

We choose the parameters A, B, C to satisfy

$$(5.1) \quad C < B, \quad 2B < A.$$

This surface S is illustrated in Figure 5.1. In all of our examples, we use $(A, B, C) = (5, 2, 1)$.

A surprising number of phenomena can be studied with the use of this quite simple surface.

- S contains ‘shadow lines’. More precisely, S_1 has shadow lines along the boundaries of the squares $[0, 2B - C] \times [0, 2B - C]$ and $[0, 2B] \times [0, 2B]$; cf. Figure 5.2. Therefore one can study the effects of ‘discontinuity meshing’ (cf. [16]). For an analysis of this with examples for both piecewise constant and piecewise linear collocation; see [6].

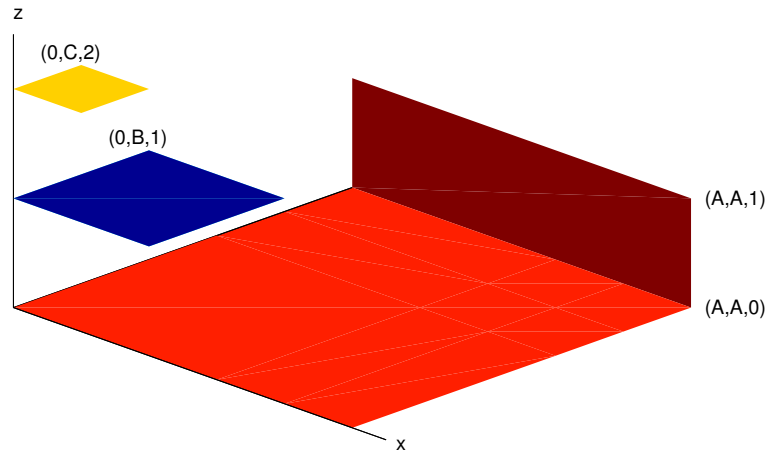


FIG. 5.1. *The 5-piece surface S*

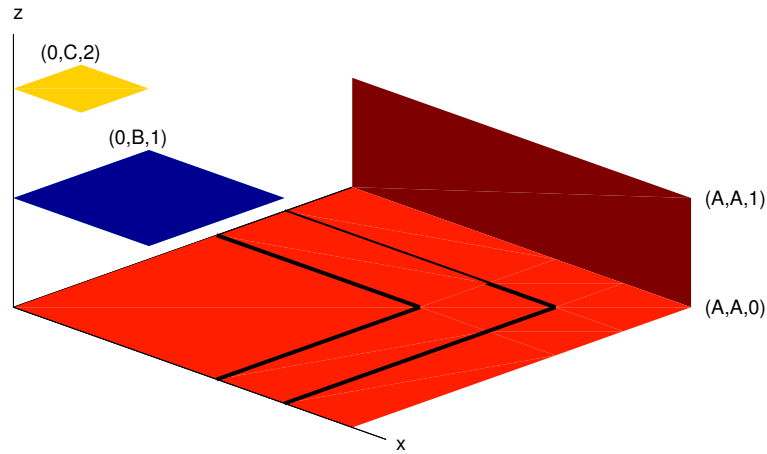


FIG. 5.2. *The 5-piece surface S with shadow lines showing*

- S is an occluded surface. For example, S_3 cannot be seen from any portion of either S_1 or S_5 , and only portions of S_1 can be seen from S_4 . Therefore, there will be visibility lines cutting through a number of elements.
- There will usually be singular behaviour in the radiosity solution along the common edge of S_1 and S_5 . See [18] for an analysis of this singular behaviour. There is also singular behaviour associated with vertices of S , as with the endpoints of $S_1 \cap S_5$; cf. [14].
- For collocation points P near to the common edge of S_1 and S_5 , the collocation integrals are nearly singular for those triangular elements near to the collocation point,

but on the opposite sub-surface. Examples are given in [6] along with a numerical scheme for the accurate and efficient evaluation of such integrals. Analytic methods for evaluating these integrals are discussed at length in [19], [20].

We could use more complicated and physically realistic surfaces, but our surface S is sufficient for studying the principal mathematical questions we have in regard to the cost of the clustering method. To use a physically realistic surface would have required constructing a visibility complex for the surface, a nontrivial task that would have greatly complicated our programming without adding any additional insight on the questions we are studying.

5.1. Test solutions. We have carried out tests for a variety of true solutions u . In these cases, we calculate the emissivity E using highly accurate numerical integration. Then the collocation procedure is applied to find the approximate solution u_n , which is then compared to the known true solution u . In this paper we report on only two cases.

- u is constant over each sub-surface S_j , $j = 1, \dots, 5$. The collocation error is zero and thus we have the exact solution of the discretized linear system (2.9). We can compare it to the solution obtained using the clustering method, thus measuring the effect of various approximations involved in clustering.
- The significance of the shadow lines in S_1 is that the first partial derivative of u is often discontinuous when the derivative is in a direction perpendicular to the shadow line. This affects the accuracy of the approximation $\mathcal{P}_n u \approx u$. To study this phenomena, we use the following true solution u :

$$(5.2) \quad u(x, y, z) = \begin{cases} \psi_\gamma(x, y) \left[\left(\frac{x}{A}\right)^2 + \left(\frac{y}{A}\right)^3 \right] & (x, y, z) \in S_1 \\ \times [(2B - x)_+ (2B - y)_+]^\beta, & (x, y, z) \in S_2 \cup S_3 \cup S_4 \\ 1, & (x, y, z) \in S_2 \cup S_3 \cup S_4 \\ 0, & (x, y, z) \in S_5, \end{cases}$$

$$\psi_\gamma(x, y) = e^{-\gamma(2B-x)(2B-y)}.$$

The function ψ_γ is used to decrease the size of $u(x, y, 0)$ away from the shadow line on the boundary of $[0, 2B] \times [0, 2B]$. The quantity $(f)_+$ is equal to f if $f \geq 0$, and it equals zero if $f < 0$. The exponent $\beta \geq 0$. With $\beta = 1$, we have a continuous nonlinear function which has bounded, but some discontinuous first order partial derivatives along the boundary of $[0, 2B] \times [0, 2B]$. With $\beta = \frac{1}{2}$, we have an algebraic singularity along this boundary, and we can study the effects of different types of triangulations for such a solution function. We choose $u \equiv 0$ on both S_5 and on the subset of S_1 outside of the square $[0, 2B] \times [0, 2B]$. We have also forced the function u to be non-symmetric over S_1 , to lessen any special effects associated with the symmetry of the various sub-surfaces.

In all cases we use $\rho \equiv \text{constant} \leq 1$. Choosing $\rho = 1$ does not present a problem, as we still have $\|\mathcal{K}\| < 1$ due to S not being a closed surface. The cases we present here are sufficient for illustrating the fast matrix-vector multiplication method of this paper. Additional studies on the accuracy of piecewise constant and piecewise linear collocation are given in [6].

5.2. Computing. We use the basic framework of [1, §5.1]; and to implement it we use the software given in [2], with the addition of codes to implement the fast matrix-vector multiplication described in §3.1.

The timings were done on a *Dell PowerEdge 6650 workstation*. This computer has four 2.0Ghz/2MB Cache Xeon processors with 12 GB RAM. The computer was networked, but otherwise was restricted to only the given program being timed, except that we might run the program for up to three data sets simultaneously. Based on the clustering method described in §3, three lists of triangles are created: *far field*, *gray field*, and *near field*. These lists are very large, along with the lists of integrals for the gray and near fields. Our computer RAM memory cannot hold all of them, so a cache scheme is used to store the lists for rapid retrieval during the iteration phase.

6. Experimental results. The central questions involve the cost of our method for the radiosity equation on an occluded surface. We begin by looking at the number of quantities in the near field, gray field, and far field. Let $\sigma(P_i)$ denote the number of admissible clusters in the far field for the point P_i , and

$$\sigma_F = \max_{P_i} \sigma(P_i).$$

Define σ_N and σ_G similarly, for the near field and the gray field as P_i ranges over the collocation nodes. From Theorems 4.4 and 4.5,

$$(6.1) \quad \sigma_F \leq C_F \eta^{-\omega} \log[2 + \eta^\omega n]$$

$$(6.2) \quad \sigma_N \leq C_N \eta^{-\omega}$$

with constants C_F, C_N that are independent of η and n . From (4.10) and (4.11) we know $\omega \leq 2$; below we examine its size empirically. Note that these formulas depend on η , not on the degree of the Taylor expansion used in approximating G in the far field. In addition for a uniform triangulation scheme (as we are using), it is straightforward to show that

$$(6.3) \quad \sigma_G \leq C_G \sqrt{n}.$$

The constant C_G is independent of η .

We give empirical results for (6.1)-(6.3) as both η and n vary, beginning with the gray field. Table 6.1 contains results for σ_G , and as we noted the results do not depend on η .

TABLE 6.1
Values of σ_G for varying n

| | | | | | | | | |
|------------|----|----|-----|-----|------|-------|-------|--------|
| n | 10 | 40 | 160 | 640 | 2560 | 10240 | 40960 | 163840 |
| σ_G | 2 | 6 | 14 | 28 | 60 | 118 | 248 | 508 |

In Figure 6.1, we give a log-log graph of n vs. σ_G , together with a linear least squares fit to determine experimentally the value of θ in

$$\sigma_G = c n^\theta.$$

The value obtained with a fit to the values $160 \leq n \leq 163840$ is $\theta \doteq .519$, which is consistent with the theoretically expected value of 0.5 from (6.3).

For the near field, we give values of σ_N for varying n and η in Table 6.2, and a log-log graph of σ_N vs. n is given in Figure 6.2. The upper bound in (6.2) is independent of n ; and

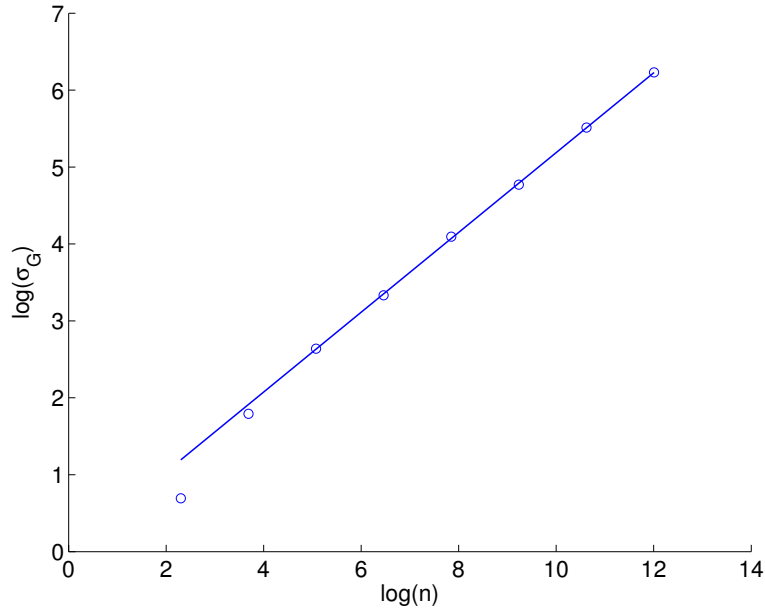


FIG. 6.1. Gray field values of σ_G and linear fit to log-log graph of values.

TABLE 6.2
 Values of σ_N for varying n and η

| n | σ_N | | |
|--------|---------------|----------------|-----------------|
| | $\eta = .125$ | $\eta = .0625$ | $\eta = .03125$ |
| 10 | 6 | 6 | 6 |
| 40 | 16 | 24 | 24 |
| 160 | 70 | 78 | 96 |
| 640 | 128 | 300 | 334 |
| 2560 | 232 | 508 | 1206 |
| 10240 | 262 | 922 | 2022 |
| 40960 | 262 | 1044 | 3700 |
| 163840 | 262 | 1044 | 4184 |

for the larger values of n (with $\eta = .0625$ and $\eta = .03125$), we have that σ_N is independent of n as well.

A table of values σ_F for the far field are given in Table 6.3. To look at the values graphically, we consider the theoretical formula of (6.1). We graph the values of $\log n$ vs. $\eta^\omega \sigma_F$, as then the theory would say

$$\begin{aligned}
 \eta^\omega \sigma_F &\approx C_F \log [2 + \eta^\omega n] \\
 (6.4) \qquad &\approx C_F [\omega \log \eta + \log n]
 \end{aligned}$$

and the graph should be linear. The graphical results are shown in Figure 6.3 with $\omega = 1.55$ rather than the theoretical value of $\omega = 2$. The results do show straight lines, approximately, for larger values of n , and they are parallel for varying values of η , as would be predicted by

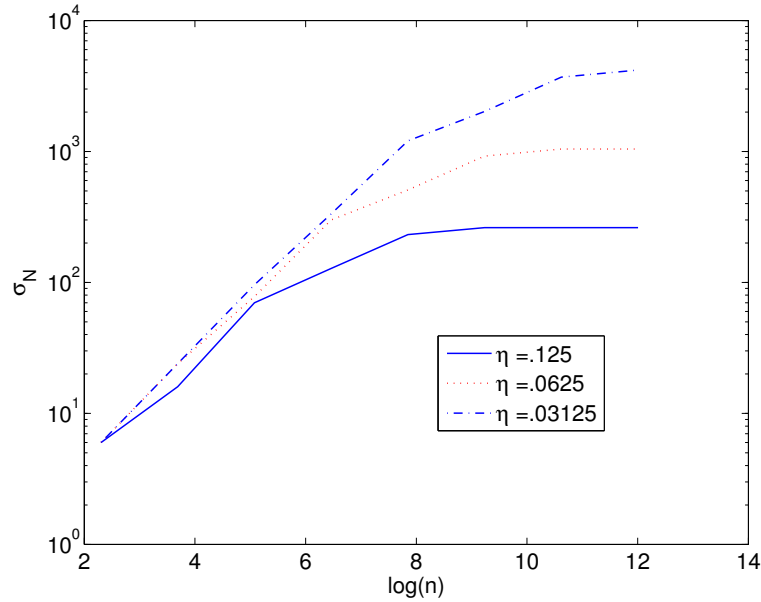


FIG. 6.2. The near field values of σ_N for varying n and η

TABLE 6.3
 Values of σ_F for varying n and η

| n | σ_F | | |
|--------|---------------|----------------|-----------------|
| | $\eta = .125$ | $\eta = .0625$ | $\eta = .03125$ |
| 10 | 2 | 0 | 0 |
| 40 | 8 | 8 | 0 |
| 160 | 60 | 32 | 32 |
| 640 | 248 | 256 | 128 |
| 2560 | 670 | 972 | 1034 |
| 10240 | 1116 | 2686 | 3860 |
| 40960 | 1824 | 4464 | 10878 |
| 163840 | 2598 | 7242 | 17754 |

(6.4). To determine the experimental value of $\omega = 1.55$, we observed the variation of σ_F vs. η for $n = 163840$ and we attempted to fit it based on the Hackbush model of (6.1) with a suitable value of ω . The results, using a log-log scale, are shown in Figure 6.4 for $\omega = 1.55$. and there is close agreement for smaller values of η .

6.1. Testing the program. By using a solution u that is constant or linear over each sub-surface S_j , the true collocation solution u_n equals u , and the true error in the numerical method based on §3.1 satisfies

$$(6.5) \quad u - \tilde{u}_n = u_n - \tilde{u}_n.$$

This allows testing the effects of the other sources of error in the numerical method. In this case the remaining error in solving the radiosity equation using the collocation method with

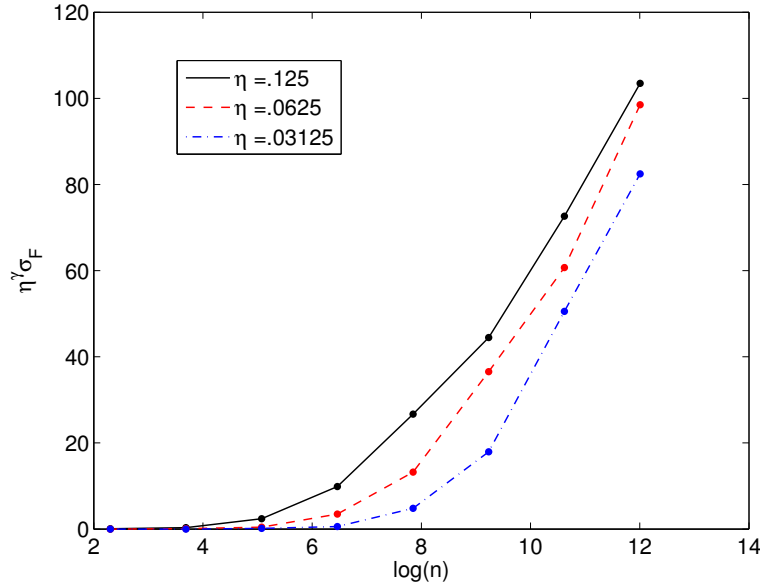


FIG. 6.3. The number of elements in the far field, normalized by η^ω .

the fast matrix-vector multiplication method of §3 is due to the following.

- The approximation $K_n \approx \tilde{K}_n$.
- Numerical integration errors for the near field and the gray field collocation integrals (cf. (2.9))

$$(6.6) \quad \int_{\Delta_j} V(P_i, Q)G(P_i, Q)\varphi_{k_j, \ell}(Q) dS_Q.$$

- Integration errors in computing the right hand emissivity function

$$(6.7) \quad E(P) = u(P) - \frac{\rho(P)}{\pi} \int_S u(Q)G(P, Q)V(P, Q) dS_Q, \quad P \in S,$$

for the given known solution u . Of course, in actual graphics computations this is not a difficulty since E is given explicitly.

The numerical integration errors for (6.6) and (6.7) can be quite difficult to control, especially when integrating over a sub-surface S_j with the field point $P \in S_k$, $k \neq j$, and P near to a common edge joining S_j and S_k . The numerical integration methods used here are discussed in [6].

To illustrate the effects of these possible errors for our numerical method, we used the true solution

$$(6.8) \quad u(x, y, z) = \begin{cases} 1, & (x, y, z) \in S_1, \\ 0, & (x, y, z) \in S_2 \cup S_3 \cup S_4 \cup S_5. \end{cases}$$

In order to study the effect of the fast matrix-vector multiplication method of §3.1, the integrations of (6.6) and (6.7) were carried out to very high accuracy. Thus the only source of

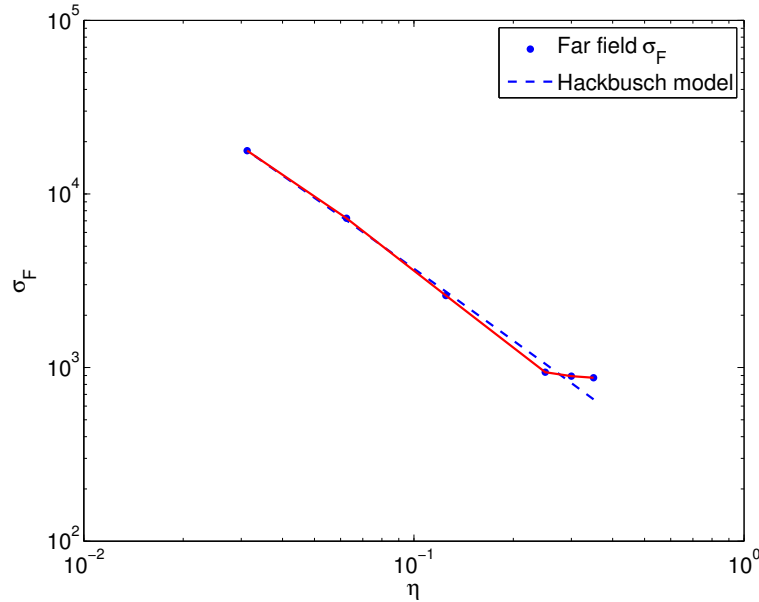


FIG. 6.4. The model (6.1) with $\omega = 1.55$, and its comparison with the graph of η vs. σ_F .

TABLE 6.4
The errors E_N for (6.8) with $\eta = 0.5$

| n | \tilde{E}_N | | |
|--------|---------------|-----------|-----------|
| | order = 2 | order = 4 | order = 6 |
| 40 | 6.54E-04 | 1.16E-04 | 2.41E-05 |
| 160 | 3.39E-03 | 3.22E-04 | 2.75E-05 |
| 640 | 2.35E-03 | 3.17E-04 | 3.59E-05 |
| 2560 | 2.77E-03 | 3.13E-04 | 5.28E-05 |
| 10240 | 2.81E-03 | 3.18E-04 | 5.27E-05 |
| 40960 | 2.81E-03 | 3.19E-04 | 5.28E-05 |
| 163840 | 2.82E-03 | 3.19E-04 | 5.28E-05 |

error in the quantity $u_n - \tilde{u}_n$ of (6.5) is the approximation $K_n \approx \tilde{K}_n$, which depends on both the Taylor order m and the far-field parameter η . Tables 6.4-6.6 give the maximum for $u_n - \tilde{u}_n$ at the collocation nodes for three values of η and for orders $m = 2, 4, 6$. Because the region is symmetric in (x, y) and the solution is also symmetric (being constant), the numerical results for orders $m = 1, 3, 5$ are the same as those for orders $m = 2, 4, 6$, respectively. In the tables,

$$(6.9) \quad \tilde{E}_N = \max_{i=1, \dots, 3n} |u_n(P_i) - \tilde{u}_n(P_i)|$$

with $\{P_i \mid 1 \leq i \leq 3n\}$ the interpolation nodes for the triangulation and u_n the true collocation solution of (6.8). This type of example gives some idea of the error to be expected when dealing with an unknown function u .

TABLE 6.5
The errors E_N for (6.8) with $\eta = 0.125$

| n | \tilde{E}_N | | |
|--------|---------------|-------------|-------------|
| | $order = 2$ | $order = 4$ | $order = 6$ |
| 40 | 9.88E-16 | 9.88E-16 | 9.88E-16 |
| 160 | 2.87E-15 | 2.87E-15 | 2.87E-15 |
| 640 | 5.17E-05 | 1.98E-07 | 1.78E-09 |
| 2560 | 1.83E-04 | 8.06E-07 | 2.90E-09 |
| 10240 | 1.25E-04 | 7.58E-07 | 3.31E-09 |
| 40960 | 1.27E-04 | 7.57E-07 | 4.44E-09 |
| 163840 | 1.29E-04 | 7.60E-07 | 5.31E-09 |

TABLE 6.6
The errors E_N for (6.8) with $\eta = 0.03125$

| n | \tilde{E}_N | | |
|--------|---------------|-------------|-------------|
| | $order = 2$ | $order = 4$ | $order = 6$ |
| 40 | 9.88E-16 | 9.88E-16 | 9.88E-16 |
| 160 | 2.87E-15 | 2.87E-15 | 2.87E-15 |
| 640 | 2.68E-15 | 2.68E-15 | 2.68E-15 |
| 2560 | 5.70E-09 | 7.33E-12 | 6.68E-15 |
| 10240 | 3.14E-06 | 6.69E-10 | 3.71E-13 |
| 40960 | 1.11E-05 | 3.10E-09 | 5.53E-13 |
| 163840 | 7.57E-06 | 2.89E-09 | 6.86E-13 |

We want to illustrate and confirm experimentally the result (4.4) in Theorem 4.1, looking at the error $(K_n - \tilde{K}_n)\mathbf{u}_n$ when it is regarded as a function of the parameter η for various values of the Taylor order m . Let $n = 163840$, and consider using the orders $m = 2, 4$ (degrees $m - 1 = 1, 3$) for our Taylor expansion in the far field. The numerical results are given in Table 6.7, and empirically they imply

$$(6.10) \quad \|\mathbf{u}_n - \tilde{\mathbf{u}}_n\|_\infty = O(\eta^m), \quad m = 2, 4.$$

From Theorem 4.1, fixing both n , the number of elements, and $m - 1$, the degree of the Taylor expansion,

$$(6.11) \quad \|(K_n - \tilde{K}_n)\mathbf{u}_n\|_\infty = O((2\eta)^m).$$

When we combine (4.4) and (6.10), we have that the theoretical rates of convergence to zero of $u_n - \tilde{u}_n$ agree with the experimental results given in Table 6.7 and (6.10).

In order for (6.11) to be consistent with the earlier bound (3.11), the value of η must be chosen so that $(2\eta)^m = O(h^\kappa)$. This results in a relation between η , n , κ , and m ,

$$\eta = O\left(n^{-\kappa/2m}\right);$$

cf. [12, Lemma 5.2]. Our experimental results imply that it is probably better to experiment with various choices of m and η for cases in which the solution is known. Then choose values of m and η so as to give sufficient accuracy while also minimizing the operations cost. We further illustrate this in the following subsection.

TABLE 6.7
The error (6.5) as a function of η

| η | <i>order = 2</i> | | <i>order = 4</i> | |
|---------|---|-------|---|-------|
| | $\ \mathbf{u}_n - \tilde{\mathbf{u}}_n\ $ | Ratio | $\ \mathbf{u}_n - \tilde{\mathbf{u}}_n\ $ | Ratio |
| 0.5 | 2.82E-3 | | 3.19E-4 | |
| 0.25 | 5.89E-4 | 4.79 | 1.34E-5 | 23.8 |
| 0.125 | 1.29E-4 | 4.57 | 7.60E-7 | 17.6 |
| 0.0625 | 3.03E-5 | 4.26 | 4.69E-8 | 16.2 |
| 0.03125 | 7.57E-6 | 4.00 | 2.89E-9 | 16.2 |

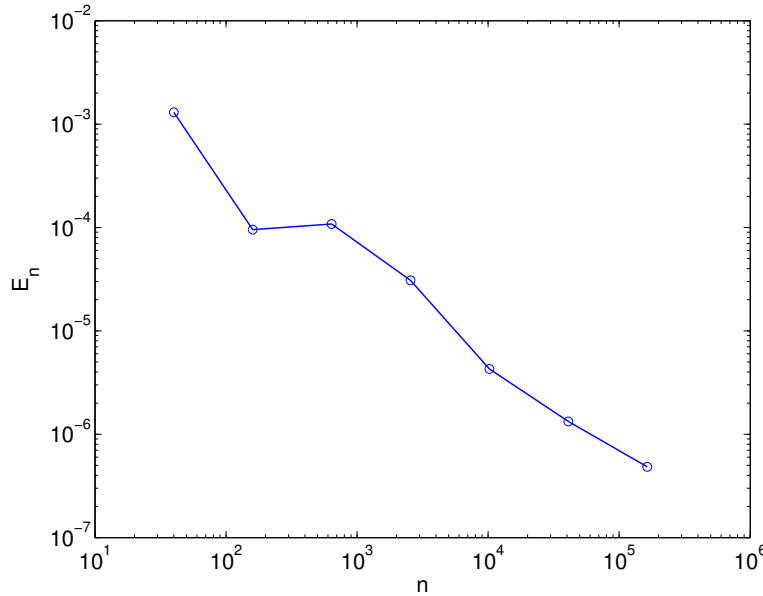


FIG. 6.5. Maximum errors in linear collocation solution.

6.2. Convergence results. We consider the numerical solution of the radiosity equation when the true solution u is chosen as in (5.2) with $\beta = 1$, $\gamma = 1.5$, and $\rho = 0.1$. We have chosen a smaller value of ρ in order to accelerate the convergence of the iteration in (2.11); but the average cost of the individual iterates is not affected by this choice of ρ . We begin with the uniform triangulation of the surface, leading to the number n of triangles as listed in the preceding Tables 6.1-6.3. With this triangulation of the sub-surface S_1 , the shadow lines of Figure 5.2 will intersect with some of the triangular elements. As in (6.9), we evaluate the error at the collocation nodes; define

$$E_N = \max_{i=1, \dots, 3n} |u(P_i) - u_n(P_i)|.$$

These maximum errors are given in Table 6.8, and they are illustrated graphically in Figure 6.5. Note that for a given number n of elements, the order of the approximating linear system equals $3n$.

Although the ratios by which the errors decrease show a great deal of variation, the

TABLE 6.8
Maximum errors in linear collocation solution

| n | E_N | <i>Ratio</i> |
|--------|---------|--------------|
| 40 | 1.30E-3 | |
| 160 | 9.53E-5 | 13.6 |
| 640 | 1.08E-4 | 0.88 |
| 2560 | 3.08E-5 | 3.51 |
| 10240 | 4.28E-6 | 7.20 |
| 40960 | 1.33E-6 | 3.22 |
| 163840 | 4.84E-7 | 2.75 |

TABLE 6.9
Errors for $\eta = 0.5$

| n | E_N | | | <i>Iteration time (seconds)</i> | | |
|--------|------------------|------------------|------------------|---------------------------------|------------------|------------------|
| | <i>order = 1</i> | <i>order = 3</i> | <i>order = 5</i> | <i>order = 1</i> | <i>order = 3</i> | <i>order = 5</i> |
| 40 | 1.38E-03 | 1.31E-03 | 1.30E-03 | .0020 | .0025 | .0035 |
| 160 | 1.17E-03 | 2.01E-04 | 9.67E-05 | .0125 | .0140 | .0220 |
| 640 | 1.41E-03 | 2.69E-04 | 1.64E-04 | .0660 | .0755 | .1315 |
| 2560 | 1.40E-03 | 2.67E-04 | 2.33E-04 | .5720 | .6085 | .7070 |
| 10240 | 1.41E-03 | 2.79E-04 | 2.71E-04 | 3.45 | 2.516 | 4.168 |
| 40960 | 1.41E-03 | 2.90E-04 | 2.80E-04 | 19.42 | 16.84 | 27.85 |
| 163840 | 1.41E-03 | 2.94E-04 | 2.86E-04 | 110.6 | 121.5 | 133.8 |

overall trend is more uniform, as is indicated in Figure 6.5. If we use the values of E_n for $n \geq 640$, we obtain an empirical rate of convergence of

$$E_n = O(n^{-p})$$

with $p \doteq 1.007$. From (2.1)-(2.4), $n^{-1} = O(h^2)$, and this leads to

$$E_n \approx O(h^2).$$

This is the expected rate of convergence for a linear collocation method, even though u is not continuously differentiable over S_1 . For a further discussion, see [6].

The error $\|u - \tilde{u}_n\|$ varies with n , η , and m . To give some insight, we give values in Tables 6.9-6.11 for

$$E_N = \max_{i=1, \dots, 3n} |u(P_i) - \tilde{u}_n(P_i)|$$

for selected values of the far field parameter η and the Taylor order m . We also give the average time (in seconds) for each iteration (as described in §2.3).

The case with parameter values of $\eta = .03125$ and order $m = 3$ (degree $m - 1 = 2$) give completely sufficient accuracy up through $n = 163840$. Using an order $m > 3$ gave essentially no additional accuracy. For smaller values of n , we can use larger values of η . For example, with $n \leq 10240$, we can have essentially the same accuracy with $\eta = .0625$, although we do not give those values here for reasons of space.

To look at the cost, we show in Figure 6.6 the average iteration time as a function of η , for varying values of Taylor approximation order m . This is done for $n = 163840$, and there are similar graphs for smaller values of n . Experimentally, the time $T \equiv T(\eta; m, n)$ satisfies

$$(6.12) \quad T \approx c_{eta}(m, n) \eta^{-p}$$

TABLE 6.10
Errors for $\eta = 0.125$

| n | E_N | | | Iteration time (seconds) | | |
|--------|-----------|-----------|-----------|--------------------------|-----------|-----------|
| | order = 1 | order = 3 | order = 5 | order = 1 | order = 3 | order = 5 |
| 40 | 1.30E-03 | 1.30E-03 | 1.30E-03 | .0037 | .0040 | .0037 |
| 160 | 1.05E-04 | 9.53E-05 | 9.53E-05 | .0417 | .0420 | .0437 |
| 640 | 1.02E-04 | 1.08E-04 | 1.08E-04 | .3440 | .3733 | .4270 |
| 2560 | 7.11E-05 | 3.11E-05 | 3.10E-05 | 2.117 | 2.377 | 2.905 |
| 10240 | 7.14E-05 | 8.58E-06 | 8.66E-06 | 10.65 | 12.19 | 15.50 |
| 40960 | 7.14E-05 | 1.09E-05 | 1.10E-05 | 51.23 | 58.56 | 74.06 |
| 163840 | 7.14E-05 | 1.05E-05 | 1.07E-05 | 259.9 | 294.5 | 364.6 |

TABLE 6.11
Errors for $\eta = 0.0625$

| n | E_N | | | Iteration time (seconds) | | |
|--------|-----------|-----------|-----------|--------------------------|-----------|-----------|
| | order = 1 | order = 3 | order = 5 | order = 1 | order = 3 | order = 5 |
| 40 | 1.30E-03 | 1.30E-03 | 1.30E-03 | .0040 | .0040 | .0043 |
| 160 | 9.53E-05 | 9.53E-05 | 9.53E-05 | .0593 | .0603 | .0610 |
| 640 | 1.08E-04 | 1.08E-04 | 1.08E-04 | .8140 | .8093 | .8253 |
| 2560 | 3.11E-05 | 3.08E-05 | 3.08E-05 | 10.05 | 10.15 | 10.71 |
| 10240 | 4.37E-06 | 4.28E-06 | 4.28E-06 | 87.63 | 99.34 | 112.2 |
| 40960 | 4.44E-06 | 1.33E-06 | 1.33E-06 | 622.5 | 748.7 | 891.2 |
| 163840 | 4.45E-06 | 4.84E-07 | 4.84E-07 | 3301 | 3923 | 4894 |

with the experimental value $p \doteq 1.88$. This is consistent with the sizes for σ_F and σ_N given in (6.1) and (6.2), and of course, σ_G depends on only n and is independent of both m and η . In the graph we also see that the time increases as the order m increases, which is to be expected. The large increases in calculation time are associated with decreasing the size of η rather than with increasing the order m .

In Figure 6.7 we show the growth of time as a function of n for varying values of η . From this log-log graph it is clear that the rate of increase is a power law in n for larger values of n . Using the case of $\eta = 0.03125$, we obtain that

$$(6.13) \quad T \approx c_{nodes}(\eta, m) n^q$$

with $q \doteq 1.19$. This is better than the worst case scenario of (3.12) which predicted an overall cost of $O(n^{1.5})$. For our values of n and η , it appears that the cost arising from treating the far field and near field is much larger and more significant than is that for the gray field.

Summary. We have examined the cost of the clustering method of Hackbusch and Nowak [12], both analytically and empirically. The empirical results agree with the form of the theoretical growth formulas given in §4, while experimentally these formulas have somewhat smaller exponents as regards the cost; this is illustrated in (6.12) and (6.13). The experimental timings also show that it is important to determine adequate values of m and η , for example, by proceeding as we did in subsections 6.1 and 6.2 with known true solutions. Too small a value of η or too large a value of m will lead to unnecessary calculation and greatly increased computation times, as is illustrated in Tables 6.9-6.11.

The clustering method allows the setup and solution of the discretized radiosity equation with a very large number of elements. In our examples, the number of equations to be set up

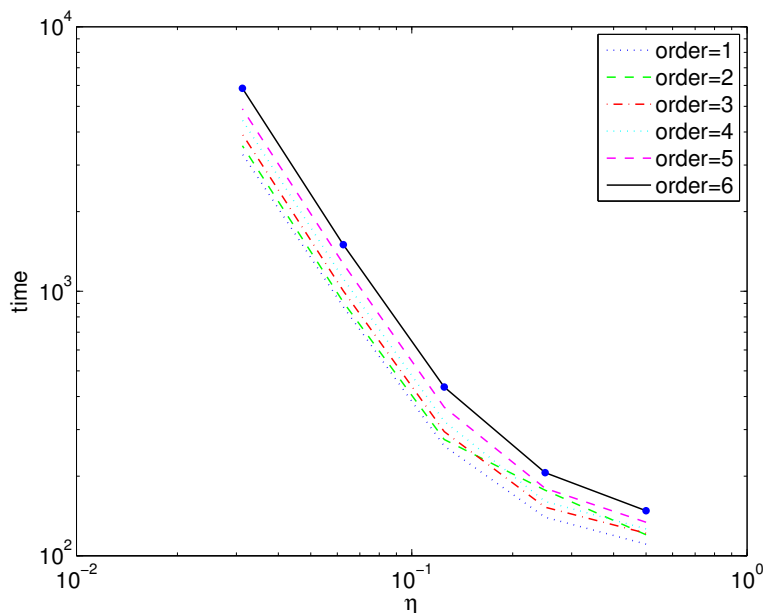


FIG. 6.6. Time as a function of η , for varying values of Taylor approximation order.

and solved is $3n$, with n the number of elements being as large as 163840 in our examples, i.e. 491520 equations. We believe this illustrates the potential importance of this method.

REFERENCES

- [1] K. ATKINSON, *The Numerical Solution of Integral Equations of the Second Kind*, Cambridge University Press, 1997.
- [2] K. ATKINSON, *User's Guide to a Boundary Element Package for Solving Integral Equations on Piecewise Smooth Surfaces*, (Release #2), Reports on Computational Mathematics #103, Dept of Mathematics, University of Iowa, Iowa City, 1998. Programs and guide are available at <http://www.math.uiowa.edu/~atkinson/bie.html>.
- [3] K. Atkinson, *The planar radiosity equation and its numerical solution*, IMA J. Numer. Anal., 20 (2000), pp. 303–332.
- [4] K. Atkinson and G. Chandler, *The collocation method for solving the radiosity equation for unoccluded surfaces*, J. Integral Equations Appl., 10 (1998), pp. 253–290.
- [5] K. ATKINSON AND D. CHIEN, *A fast matrix-vector multiplication method for solving the radiosity equation*, Adv. Comput. Math., 12 (2000), pp. 151–174.
- [6] K. ATKINSON, D. CHIEN, AND J. SEOL, *Numerical analysis of the radiosity equation using the collocation method*, Electron. Trans. Numer. Anal., 11 (2000), pp. 94–120, <http://etna.math.kent.edu/vol.11.2000/pp94-120.dir/pp94-120.html>.
- [7] M. CHEN AND J. ARVO, *A closed-form solution for the irradiance due to linearly-varying luminaries*, in Proceedings of the Eleventh Eurographics Workshop on Rendering, Brno, Czech Republic, June 2000, pp. 137–148.
- [8] M. CHEN AND J. ARVO, *Simulating non-Lambertian phenomena involving linearly-varying luminaries*, in Proceedings of the Twelfth Eurographics Workshop on Rendering, London, June 2001.
- [9] M. COHEN AND J. WALLACE, *Radiosity and Realistic Image Synthesis*, Academic Press, New York, 1993.
- [10] G. COOMBE, M. HARRIS, AND A. LASTRA, *Radiosity on graphics hardware*, in Proceedings of the 2004 Conference on Graphics Interface, ACM International Conference Proceeding Series, Vol. 62, ACM Press, 2005, pp. 161–168.

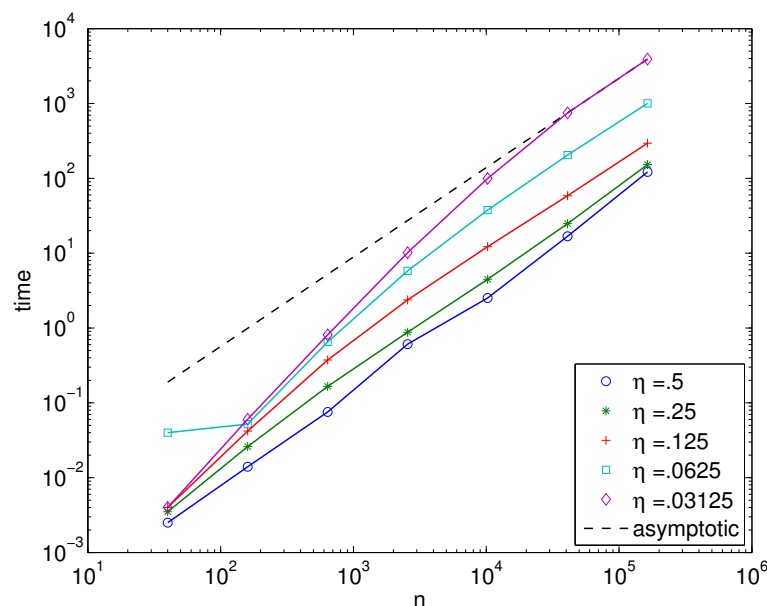


FIG. 6.7. The number of elements n vs. the average iteration time in seconds, for varying η .

- [11] S. GORTLER, P. SCHRÖDER, M. COHEN, AND P. HANRAHAN, *Wavelet radiosity*, in Proceedings of the 20th Annual Conference on Computer Graphics and Interactive Techniques, ACM Press, 1993, pp. 221–230.
- [12] W. HACKBUSCH AND Z. NOWAK, *On the fast matrix multiplication in the boundary element method by panel clustering*, Numer. Math., 54 (1989), pp. 463–491.
- [13] P. HANRAHAN, D. SALZMAN, AND L. AUPPERLE, *A rapid hierarchical radiosity algorithm*, in Proceedings of the 18th Annual Conference on Computer Graphics and Interactive Techniques, 1991, ACM Press, pp. 197–206.
- [14] O. HANSEN, *The radiosity equation on certain spaces of continuous functions and its numerical solution*, Habilitationsschrift, Fachbereichs Mathematik, der Johannes Gutenberg-Universität Mainz, 2001.
- [15] O. HANSEN, *On the stability of the collocation method for the radiosity equation on polyhedral domains*, IMA J. Numer. Anal., 22 (2002), pp. 463–479.
- [16] D. LISCHINSKI, F. TAMPIERI, AND D. GREENBERG, *Discontinuity meshing for accurate radiosity*, IEEE Computer Graphics & Applications, 12 (1992), pp. 25–39.
- [17] S. MICULA, *Numerical methods for the radiosity equation and related problems*, PhD thesis, Univ. of Iowa, Iowa City, 1997.
- [18] A. RATHSFELD, *Edge asymptotics for the radiosity equation over polyhedral boundaries*, Math. Methods Appl. Sci., 22 (1999), pp. 217–241.
- [19] J. SEOL, *Analysis of the radiosity equation using the collocation method*, PhD thesis, Univ. of Iowa, Iowa City, 2002.
- [20] J. SEOL AND K. ATKINSON, *Numerical evaluation of collocation integrals for the radiosity equation*, Appl. Numer. Anal. Comput. Math., 2 (2005), pp. 306–325.
- [21] F. SILLION AND C. PUECH, *Radiosity and Global Illumination*, Morgan Kaufmann Pub., San Francisco, 1994.
- [22] A. STROUD, *Approximate Calculation of Multiple Integrals*, Prentice-Hall, New Jersey, 1971.